

1 Carbon isotopic evidence for organic matter oxidation in soils of the Old Red Sandstone (Silurian to  
2 Devonian, South Wales, UK).

3  
4 A.T. Brasier<sup>1\*</sup>, J.L. Morris<sup>2,3</sup>, R.D. Hillier<sup>4</sup>

5 1) Faculty of Earth and Life Sciences, VU University Amsterdam

6 2) School of Earth and Ocean Sciences, Cardiff University, Cardiff, CF10 3AT

7 3) Department of Animal and Plant Sciences, University of Sheffield, Sheffield, S10 2TN

8 4) Department of Geology, National Museums and Galleries of Wales, Cathays Park, Cardiff, CF10 3NP

9  
10 Corresponding author (email: a.t.brasier@vu.nl)

11  
12 Number of words: 10894

13 Abbreviated title: CO<sub>2</sub>-rich soils in the Siluro-Devonian

14  
15 **Abstract**

16 Petrographic and calcrete carbon isotope data from seasonally waterlogged Upper Silurian (Přídolí) to Lower  
17 Devonian (Pragian) palaeo-Vertisols of the Old Red Sandstone, South Wales, UK, are presented. The  $\delta^{13}\text{C}$   
18 values mostly range from -9 to -12‰ (VPDB), suggesting the soils were inhabited by abundant vegetation  
19 that when oxidised (perhaps with microbial assistance) resulted in CO<sub>2</sub>-rich soils. Such soils would favour  
20 calcrete precipitation through equilibration of soil zone CO<sub>2</sub> with the relatively lower atmospheric pCO<sub>2</sub>.  
21 However, reliably estimating palaeoatmospheric pCO<sub>2</sub> calculated from these carbon isotope data is a  
22 challenge.

23  
24 **Keywords:** calcrete, carbon isotopes, Silurian, Devonian, soil carbonate, palaeosols

25  
26 The physical appearances, sedimentary textures and depositional processes of soil carbonates have evolved  
27 through time, particularly through the Palaeozoic (Brasier 2011). One of the first major steps in terrestrial  
28 carbonate evolution was likely associated with the Palaeoproterozoic oxygenation of shallow marine and  
29 lacustrine environments (Brasier 2011), which led to widespread precipitation of calcium sulphates.  
30 Dissolution of highly soluble gypsum and anhydrite can lead to precipitation of less soluble calcite from  
31 terrestrial groundwaters (the 'common ion effect'). The widespread incorporation of organic matter from early

32 plants into soils has been hypothesised as the driver of a later major step in carbonate precipitation that likely  
33 took place in the Late Silurian or Early Devonian. This is because plant growth and organic matter  
34 incorporation raises soil zone pCO<sub>2</sub> via plant and microbial respiration or decay, which leads to enhanced  
35 production of carbonic acid. The latter can dissolve limestone bedrock (where present), and dissociate to form  
36 bicarbonate ions (HCO<sub>3</sub><sup>-</sup>). On the other hand, if the accumulated soil zone carbon dioxide is able to escape  
37 (perhaps during dry seasons as the soils begin to crack), and pCO<sub>2</sub> is higher than atmospheric pCO<sub>2</sub>, then  
38 outgassing of dissolved CO<sub>2</sub> can occur. This CO<sub>2</sub> loss drives an equilibrium reaction (reaction 1, below) to the  
39 right, leading to calcrete precipitation.

40



42

43 Chemical weathering of silicate bedrock via interaction with carbonic acid is a major driver in perturbations  
44 of global atmospheric carbon dioxide levels (e.g. Berner & Kothavala 2001). The importance of respiring  
45 vascular plants with well-developed root systems (that locally lower soil zone pH) and symbiotic mycorrhizal  
46 fungi to this process has often been emphasised (e.g. Algeo *et al.* 2001; Berner *et al.* 2003).

47

48 Calcrete deposition also requires a source of calcium ions. This could be local chemical weathering of  
49 carbonate or volcanic bedrock, although in the Recent soils of New Mexico, USA, the calcium is  
50 demonstrably sourced from windblown dust (Capo and Chadwick, 1999). Increased levels of silicate  
51 weathering (leading to increased calcium availability) could also have encouraged post-Middle Devonian non-  
52 marine carbonate precipitation (Brasier, 2011).

53

54 At least from the Middle Devonian onwards, vascular plants with root systems have actively encouraged  
55 calcrete (*sensu* Wright and Tucker, 1991) precipitation through evapotranspiration, and directly controlled the  
56 geochemistry of the rhizosphere (see references in Brasier 2011). The effects of earlier (Silurian to Early  
57 Devonian), pre-vascular plant organic matter on calcrete precipitation and morphology, and on silicate  
58 mineral weathering, must also be considered. It has previously been suggested that the biological productivity  
59 of microbiota prior to vascular plants was similar to that of modern soils (Yapp & Poths 1994), and that  
60 microbially-produced CO<sub>2</sub> levels may have been high in the vadose zone prior to the Silurian (Keller & Wood  
61 1993). Degassing of CO<sub>2</sub> from these soils could have produced calcite-supersaturated groundwaters before the  
62 later advent of vascular plants with roots actively engaged in the precipitation of calcrete.

63

64 Direct evidence of preserved organic matter in Late Silurian to Early Devonian terrestrial deposits is limited.  
65 The Anglo-Welsh Basin of South Wales and the Welsh Borderland (Fig. 1) has yielded an unrivalled record  
66 of early land plant history (e.g. Lang 1937; Edwards & Richardson 2004), in particular vascular plant remains  
67 such as *Cooksonia* (Edwards 1979). The majority of megafossil remains are allochthonous in nature, although  
68 downward-bifurcating drab haloes are common in palaeosols, and have been interpreted as surface water  
69 gleying around small-scale rooting structures that subsequently decayed (Allen 1986; Allen & Williams, 1982).  
70 Hillier *et al.* (2008) described shallow rooting structures from a wide range of terrestrial environments across  
71 the basin, and used circumstantial evidence to conclude that these structures could have been produced by the  
72 fungus *Prototaxites*. In addition to rooting structures, the Late Silurian to Early Devonian terrestrial deposits  
73 preserved a diverse ichnofauna that demonstrates a complex trophic structure (Morrissey *et al.* 2012).  
74 “Enigmatic” sedimentary structures such as millimetre-scale ripples and wrinkle structures provide evidence  
75 for widespread microbial presence around palaeosols and their spatially associated environments, constituting  
76 a plausible base to the trophic pyramid (Morrissey *et al.* 2012; Marriott *et al.* 2012).

77

78 Many Late Silurian to Early Devonian palaeosols from the Anglo-Welsh Basin contain abundant calcrite  
79 nodules (e.g. Allen 1974; Marriott & Wright 1993; Love & Williams 2000; Hillier *et al.* 2011a). The aim of  
80 this study was to test the possibility of a link between the palaeontological and sedimentary evidence for  
81 terrestrial biological activity, organic matter accumulation and the occurrence of these early calcrite nodules.  
82 Processes that could have caused the calcrite precipitation include evaporation, the common-ion effect, or  
83 loss of CO<sub>2</sub> from the soil to the relatively lower *p*CO<sub>2</sub> atmosphere (via reaction 1). Evidence for  
84 predominance of the latter process would suggest that Late Silurian to Early Devonian terrestrial organisms  
85 (either actively when alive or passively when dead) produced high *p*CO<sub>2</sub>, carbonic acid rich soils prior to the  
86 evolution of deeper-rooted plants.

87

88 Calcrite carbon isotope geochemistry should portray the influence of soil zone organic matter on calcrite  
89 precipitation. Carbon isotope data from pre-Silurian calcrites are currently scarce, but values reported to date  
90 are all much closer to 0‰ VPDB than found in more recent examples. These ancient cases include the  
91 Cambrian La Flecha Formation calcrites of Argentina (-1 to -3‰; Keller *et al.*, 1989; Buggisch *et al.*, 2003),  
92 and Cambrian alluvial fan calcrites of the Guaritas Sequence of Brazil (-1.47 to -0.99‰; De Ros *et al.*, 1994).  
93 Their relatively positive carbon isotope compositions likely reflect a very small or negligible contribution of

94 biologically processed carbon to pre-Silurian soil zone CO<sub>2</sub>. In contrast, Late Devonian to modern calcrete  
95 δ<sup>13</sup>C values are mostly strongly negative (e.g. Ekart et al., 1999). Their signals are dominated by CO<sub>2</sub> respired  
96 by soil-inhabiting organisms, in addition to the CO<sub>2</sub> resulting from oxidation of dead soil zone organic matter  
97 (e.g. Cerling 1984; Driese & Mora 1993; Mora *et al.* 1996; Ekart *et al.* 1999). If organic matter oxidation in  
98 the Late Silurian and Early Devonian produced high soil zone pCO<sub>2</sub>, facilitating and accelerating widespread  
99 calcrete precipitation via reaction 1, and potentially enhancing silicate bedrock weathering, this should be  
100 reflected in the calcrete δ<sup>13</sup>C record.

101

## 102 **Geological setting**

103

### 104 *Basin History*

105 The Old Red Sandstone magnafacies outcrops across South Wales and the Welsh Borderland, U.K. (Fig. 1)  
106 and comprises predominantly terrestrial sequences that were deposited in the Anglo-Welsh Basin during the  
107 Late Silurian to Early Carboniferous. During this interval the basin lay on the southern margins of Laurussia  
108 within sub-tropical latitudes (c. 17° S; Channell *et al.* 1992; Friend *et al.* 2000). The Lower Old Red  
109 Sandstone Daugleddau Group (Fig. 2; Barclay *et al.* in press) is of Late Ludlow to Early Devonian (Emsian)  
110 age. Sequences of the lower part of the group (the Milford Haven Subgroup) were deposited mainly in  
111 dryland coastal plain and alluvial floodplain environments that developed in a semi-arid climate (Allen 1974;  
112 Barclay *et al.* 2005; Hillier & Williams 2006). Contemporaneous volcanic tuffs were likely sources of calcium  
113 for the calcretes and are interbedded throughout the succession (e.g. Marriott et al., 2009). The upper Přídolí  
114 Moor Cliffs Formation is a mudstone-dominated, heterolithic succession of moderately sinuous ephemeral  
115 river channel and floodplain deposits that were pedified to varying degrees as calcic palaeo-Vertisols, of  
116 which the C horizons are often defined by the presence of pedogenic calcrete (as further described  
117 below; Allen & Williams 1979; Marriott & Wright 1993; Marriott & Wright 2004). The formation also  
118 preserves low-gradient, high width-to-depth ratio ephemeral fluvial sandbodies (Love & Williams 2000;  
119 Williams & Hillier 2004). The top of the formation is marked by the Chapel Point Limestone Member (Fig.  
120 2), a unit of well-developed stacked calcrete-containing palaeosols of significant aerial extent across the basin,  
121 which signifies a period of basin-wide sedimentary hiatus and pedogenesis close to the Silurian-Devonian  
122 boundary (Williams *et al.* 1982; Allen 1986; Wright & Marriott 1996).

123

124 A basin-wide change in palaeohydrology and geomorphology occurred across the Silurian-Devonian  
125 boundary, with the appearance of sandstone-dominated perennial fluvial channels of the lower Lochkovian  
126 Freshwater West Formation (Fig. 2). These may represent an overall wetter climate than that of the Late  
127 Silurian, possibly associated with a more intense monsoonal climate (Hillier *et al.* 2007; Morris *et al.* 2012).  
128 The presence of hydromorphic palaeosols indicates intervals of prolonged waterlogging (Hillier *et al.* 2007),  
129 the higher water table facilitating the preservation of plant micro- and macrofossils (Higgs 2004; Morris *et al.*  
130 2011, 2012). During intervals of low precipitation and discharge, the basin essentially reverted to an  
131 ephemeral dryland mudstone-dominated system with well-developed calcic palaeo-Vertisols (Hillier *et al.*  
132 2007). Most of the Late Silurian- Early Devonian deposits were derived from the north, with the exception of  
133 the late Lochkovian Ridgeway Conglomerate Formation, found south of the Ritec Fault in Pembrokeshire  
134 (Fig. 1), with deposits derived from the south. It represents an interval of transtensional related half-graben  
135 development in the basin, with increased topographic relief shedding ephemeral alluvial fan deposits into  
136 contemporaneous dryland alluvial valleys (Hillier & Williams 2007).

137

#### 138 *Pedogenic vs. groundwater calcretes*

139 The term calcrete is defined as ‘a near surface, terrestrial accumulation of predominately calcium carbonate,  
140 which occurs in a variety of forms from powdery to nodular to highly indurated’ (Lampugh 1902; Goudie  
141 1973; Wright & Tucker 1991). The term applies to carbonate accumulations in soils and palaeosols  
142 (‘pedogenic calcretes’), and also to groundwater precipitates (‘groundwater calcretes’; see Wright & Tucker  
143 1991). Much calcrete in the Old Red Sandstone of the Anglo-Welsh Basin is pedogenic. Typical pedified red  
144 beds of the Old Red Sandstone are recognised by three soil horizons that occur as single vertical profiles or,  
145 more commonly, as a series of stacked profiles with complex depositional and pedogenic histories (Allen  
146 1974, 1986; Marriott & Wright 1993, 2006). The upper (A) horizon is characterised by the presence of blue-  
147 grey vertically orientated vein-like features, ascribed by most authors to local reduction of iron (‘drab haloes’)  
148 around roots, but may also represent burrows or desiccation cracks. The middle (Bss ) horizon is recognised  
149 by the presence of convex-up, wedge shaped peds with slickensided slip-planes. The lower (Ck) horizons  
150 possess various types of pedogenic carbonate, including sub-spherical nodules, elongate, columnar rods and  
151 crystallaria, ranging from stage I to V in development (*sensu* Machette 1985). Calcrete precipitation and  
152 growth in soils is displacive.

153

154 When compared to modern soil orders (US soil taxonomy) the A-Bss-Ck horizonation is most similar to that  
155 of Vertisols (Soil Survey Staff 1999), hence most palaeosols within the Anglo-Welsh Basin are interpreted as  
156 calcic palaeo-Vertisols (e.g. Allen 1986; Marriott & Wright 1993, 2004; Love & Williams 2000). Today the  
157 majority of Vertisols develop under conditions of limited moisture, but that are sufficient for plant growth  
158 (ustic regimes; Soil Survey Staff 1999). Many authors have interpreted the pedogenic features observed as  
159 evidence for a semi-arid palaeoclimate with distinct wet and dry seasons (Allen 1986; Marriott & Wright  
160 1993, 1996, 2004). For example, shrinking and swelling of clays under such conditions leads to the formation  
161 of the slickensided slip-planes (Wilding & Tessier 1988), while pedogenic calcrete formation itself might  
162 require strong seasonality (e.g. Breecker *et al.* 2010). Seasonal wetting and drying of the soils promoted  
163 alternating periods of oxidation and reduction, and subsequent formation of redoximorphic indicators such as  
164 drab haloes around rooting traces, fractures and desiccation cracks (pseudogleying). In addition, and  
165 particularly common in the Conigar Pit Sandstone Member, is the development of red/purple and grey to  
166 grey/green colour mottling in sandstone bodies. The latter may be oval or outline depositional structures such  
167 as cross-lamination. They are interpreted as redoximorphic indicators of seasonal saturation as iron oxides  
168 were reduced (low chromas) or oxidised (high chromas) by a fluctuating water table (Hillier *et al.* 2007).  
169 Pedogenic calcretes are usually assumed to have obtained their carbon from a combination of atmospheric  
170 CO<sub>2</sub> and biological, respired CO<sub>2</sub> in the soil zone (e.g. Cerling 1984). Some re-working of carbon from older  
171 pedogenic calcrete is also to be expected in these systems.

172

173 Conversely, groundwater calcretes precipitate from mobile carbonate-rich groundwaters. These carbonates are  
174 commonly precipitated in layers within the capillary fringe zone, but they can be precipitated below the water  
175 table (Wright & Tucker 1991). They have been recognised in the Old Red Sandstone of the Anglo-Welsh  
176 Basin as sharp-based, layer-bound micritic calcretes with upper surfaces comprising vertical and cylindrical  
177 nodules (Hillier *et al.* 2011*b*). Groundwater calcretes may source their carbon from beyond the soil zone (e.g.  
178 underlying bedrock, or older pedogenic calcretes).

179

### 180 **Localities and methodology**

181 The majority of the calcretes sampled are from South-west Wales. Here there is good section exposure of  
182 recognisable, well-developed palaeosol profiles that have been extensively studied (e.g. Allen & Williams  
183 1982; Williams *et al.* 1982; Marriott & Wright 1993, 2004; Love & Williams 2000; Williams & Hillier 2004;  
184 Hillier *et al.* 2007). Palaeosol profiles of the upper Přídolí Moor Cliffs Formation were examined, and

185 carefully selected calcretes were sampled from Manorbier, Pembrokeshire (latitude 51.644212°, longitude -  
186 4.806869°) and Llansteffan, Carmarthenshire (latitude 51.752037°, longitude -4.634724°) (Fig. 1). Calcretes  
187 from the lower Lochkovian Freshwater West Formation were collected from palaeosols identified throughout  
188 the type section at Freshwater West, Pembrokeshire (latitude 51.652384°, longitude -5.057570°) and at  
189 representative shorter sections at Manorbier and Llansteffan. Samples from the late Lochkovian Ridgeway  
190 Conglomerate Formation were collected at Freshwater West.

191  
192 Additional pedogenic calcrete nodules were sampled from central South Wales, from palaeosol profiles of the  
193 lower Lochkovian Freshwater West Formation (previously known in the region as the St. Maughans  
194 Formation, Barclay *et al.* 2005, in press; Fig. 2), Chapel Point Limestone Member, and Moor Cliffs Formation  
195 (previously known regionally as the Raglan Mudstone Formation). These were all identified in two cores from  
196 Tredomen Quarry (BGS registration numbers SO13SW/2 & SO13SW/3), near Brecon, Powys (Fig. 1; latitude  
197 51.965185°, longitude -3.285985°; Morris *et al.* 2011, 2012).

198  
199 All hand-specimens were examined with a binocular microscope and stained with Alizarin Red S and  
200 Potassium Ferricyanide to enable clear distinction between calcite and dolomite. Those deemed suitable for  
201 analysis and representative of each calcrete type were thin-sectioned. Half of each thin-section was then  
202 stained with Alizarin Red S and Potassium Ferricyanide prior to examination with a petrographic microscope.  
203 Detailed information on stable isotope measurement methods is provided in the supplementary information.

204

## 205 **Results**

206

### 207 *Petrography, selection and sampling of calcretes*

208

209 A summary of petrographic observations is given here, with more detailed descriptions in the supplementary  
210 information.

211

### 212 *Moor Cliffs Formation palaeosols*

213 At Manorbier, the Moor Cliffs Formation is a thick sequence of predominantly brownish-red silty mudstones  
214 interbedded with subordinate conglomerates, tuffs and sandstone bodies (Williams *et al.* 1982; Marriott &  
215 Wright 1993, 2004; Love & Williams 2000). Marriott & Wright (1993) recognised 20 mudstone intervals that

216 indicated varying degrees of pedification. Over half of the sequences they observed are complex, truncated  
217 cumulate profiles, with only 5 truncated simple profiles recognised. All three horizons typical of palaeo-  
218 Vertisols were recognised (A-Bss-Ck). The C horizons are rich in calcrete (Fig. 3), ranging in morphology  
219 from: 5 to 10 mm diameter discrete nodules; larger calcrete ‘rods’ of 10 to 40 mm diameter and up to 150 mm  
220 long; and coalescent calcrete rods and nodules (Marriott & Wright 1993), representing stages I – III in  
221 calcrete development (*sensu* Machette 1985). Although most of the calcrete rods are orientated vertically,  
222 some are aligned along wedge-shaped ped slip planes, where overprinting of the B horizon has occurred,  
223 indicative of (syn-sedimentary) reactivation of the slip planes. A representative sample from each calcrete  
224 type or development stage was taken (Table S1). Thin-section microscopy of one of the smaller nodules (Fig.  
225 3a, 3b) reveals micrite surrounding clear, sparry calcite cement that infills irregular-shaped voids. A simple  
226 explanation of sparry calcite cementation (perhaps during burial) of burrows within siliciclastic host rock  
227 would not account for the relationship between the micrite and the spar. More likely is a two-stage process,  
228 starting with micritic calcite precipitation around an organic substrate (plants or other organisms, perhaps after  
229 their burial in the soil). Secondly the organic matter oxidized, leaving behind convolute voids, of up to 0.5  
230 mm width and several millimetres in length, within the earlier-formed micrite. All stages of calcite  
231 precipitation could have happened syn-depositionally, associated with CO<sub>2</sub> degassing from the soil zone to the  
232 atmosphere. Samples of micritic oval pellets, 0.5 cm in diameter, probably of faecal origin (Allen & Williams  
233 1981; Marriott *et al.* 2009) and calcitised horizontal burrow fills (perhaps *Beaconites barretti*; see Marriott *et*  
234 *al.* 2009), of up to 3 cm length and 0.5 cm width, were also taken (Table S1).

235

236 Calcretes from the top of the Moor Cliffs Formation were sampled from exposures at Llansteffan (Fig. 1),  
237 specifically from the Chapel Point Limestone Member (formerly the *Psammosteus* Limestone / Bishop’s  
238 Frome Limestone; see Fig. 3c and Barclay *et al.* in press). This pedogenic calcrete unit comprises aggraded  
239 well-developed (up to stage V) calcrete (C) horizons, totalling up to 20m thick (Marriott & Wright 1993;  
240 Jenkins 1998), suggesting a prolonged period of slow sedimentation and tectonic and climatic quiescence  
241 lasting many thousands of years (Allen 1974; Allen 1985; Wright & Marriott 1996; Jenkins 1998). In thin-  
242 section (Fig. 3d) these nodules exhibit typical calcrete fabrics like crystalline mosaics and circum-granular  
243 cracks that can be interpreted as primary in origin (Wright & Tucker, 1991). The mosaics and fracture-filling  
244 spar are therefore not seen as evidence for carbonate mobilisation during burial.

245

246 *Freshwater West Formation palaeosols*



247 The Conigar Pit Sandstone and Rat Island Mudstone Members of the Freshwater West Formation (Fig. 2)  
248 have been extensively described by Hillier *et al.* (2007) and Marriott & Wright (1993), respectively. The  
249 Conigar Pit Sandstone Member is the lower part of the formation and is characterised by interbedded  
250 heterolithics, sheet and multi-storey sandstones and mudstones. The mudstones represent 30% of the Conigar  
251 Pit Sandstone Member at Freshwater West, and were deposited either in shallow, ephemeral pools on the  
252 floodplain or as within-channel muddy braid bars (Hillier *et al.* 2007). Pedogenic processes have affected  
253 many of these muds (Fig. 4); the majority of the profiles recognised are cumulative. Blue-grey drab haloes,  
254 abundant within the A horizons, have been interpreted as the traces of roots, fungal hyphae or burrows (e.g.  
255 Fig. 4a, 4b; see also Hillier *et al.* 2007; Marriott & Wright 1993). Slickensided wedge-shaped peds in the B  
256 horizons (Hillier *et al.* 2007) and pedogenic calcretes are indicative of palaeo-Vertisols, although the  
257 slickensided peds are weakly-developed compared to those of the Moor Cliffs Formation. The majority of C  
258 horizons have stage I calcrete nodules, with some up to stage II-III (Hillier *et al.* 2007).

259

260 The Rat Island Mudstone Member is the upper part of the formation, containing pedified mudstones described  
261 by Marriott & Wright (1993) as weakly-developed calcic palaeo-Vertisols. They are more prevalent than  
262 those in the Conigar Pit Sandstone Member; the sandstone: mudstone ratio within the former being 1:3. The  
263 calcretes are mostly developed to stages I & II, with rare occurrences of stage III. The majority of profiles are  
264 cumulate, with only a small proportion truncated, and no evidence of reactivation (Marriott & Wright 1993).

265

266 Four forms of calcrete were collected from the Freshwater West Formation at Manorbier and Freshwater West  
267 (Fig. 1; Table S1). The first three are: large (commonly 5 cm diameter) pedogenic nodules (Fig. 4a); smaller,  
268 centimetre-sized, elongated calcrete nodules, sometimes oriented between peds (Fig. 4c); and small (up to  
269 5mm diameter) transported calcrete clasts (for example Fig. 4d) in lenses of well-sorted intraformational  
270 conglomerates, likely deposited during flash-flooding events. Conglomerate lenses are several metres in  
271 length and up to 10 cm thick. They are set in homogenous red mudstone matrices exhibiting blocky ped  
272 textures. The fourth form of calcrete is calcite-filled cracks (Fig. 4e) at Freshwater West, interpreted as  
273 pedogenic crystallaria.

274

275 Thin-sections of nodules from the Conigar Pit Sandstone Member (Fig. 5; Table S1) display clay-rich calcitic  
276 peloids amalgamated into nodules, surrounded by central calcite spar-filled irregular and circumgranular  
277 cracks, set in matrices of haematitic clays and sub-angular quartz grains (e.g. Fig. 5a). Dark micritic margins

278 to the largest cracks surround clear calcite similar to the relationship observed within the Moor Cliffs  
279 Formation nodules (Fig. 3). Here we similarly infer precipitation of micrite on an organic substrate, followed  
280 by oxidation of the organic matter and filling of the resulting void by spar. Circumgranular crack-filling spar  
281 is cut by stylolites (Fig. 5b, 5c), consistent with spar formation prior to deep burial. Within one vein in a  
282 single nodule (ATB 210810-7; Fig. 5d) were a very few crystals that did not stain with Alizarin Red that are  
283 either dolomite or siderite.

284  
285 A thin-section of a nodule collected from a conglomerate in the Freshwater West Formation at Llansteffan  
286 reveals a spherulitic texture (Fig. 5e). A c. 100 micron thick, c. 5mm long laminar calcite crust surrounding a  
287 spherulitic clast comprises three couplets of light and dark laminae (Fig. 5f). It is tempting to speculate that  
288 this combination of spherulites and tufa-like laminar crust imply initial subaerial precipitation of the nodule in  
289 association with cyanobacteria (perhaps initially in a stream?). However, an entirely abiotic, phreatic origin  
290 for these textures is also plausible (e.g. Verrecchia *et al.* 1995; Wright *et al.* 1995).

291  
292 Micritic areas of samples were targeted for stable isotope analysis. Thin-section ATB 220810-05 was selected  
293 for its relatively wide void-filling spar section (shown in Fig. 5a), and drilled using a computer-controlled  
294 micromill. Samples were obtained of the circumgranular crack-filling spar and its micritic lining, plus a  
295 micritic peloid. The few crystals of vein-filling dolomite or siderite and spatially-associated void-filling spar  
296 (Fig. 5d) were micromilled from a second thin-section (ATB 210810-7), but unfortunately samples obtained  
297 were not of sufficient size for analysis.

298

### 299 *Tredomen Quarry core palaeosols*

300 The Freshwater West and Moor Cliffs Formations also outcrop across central South Wales (Figs. 1 and 2;  
301 Allen & Dineley 1986). Both formations, including the Chapel Point Limestone Member, are recognised in  
302 two cores drilled at Tredomen Quarry (Fig. 1; Morris *et al.* 2012). The Freshwater West Formation comprises  
303 interbedded multi-channel sandstones, intraformational conglomerates, inclined and planar laminated  
304 heterolithics, and pedified mudstones. The majority of the latter are interpreted as calcic palaeo-Vertisols with  
305 A-Bss-Ck horizonation, mostly within truncated single profiles, but some are cumulate (Morris *et al.* 2012).  
306 The calcrete ranges from small (2-5mm in diameter), sparsely distributed sub-spherical micritic nodules (stage  
307 I), to larger (over 5mm in diameter) sub-spherical and elongate nodules (stage II). Two stage II-III (coalesced)  
308 calcrete horizons are interpreted as the Chapel Point Limestone Member. Underlying this are rocks of the

309 Moor Cliffs Formation, being predominately vertic and non-vertic calcic palaeosols, interbedded with inclined  
310 and planar-laminated heterolithics and minor sandstones with intraformational conglomeratic bases (Morris *et*  
311 *al.* 2012). The palaeosol profiles are commonly cumulate, often with no clear horizonation, although some  
312 truncated single profiles were observed. Pedogenic calcrete development ranges between stages I and II.

313

314 Five micritic nodules were chosen (three from the Freshwater West Formation, one from the Chapel Point  
315 Limestone Member and one from the Moor Cliffs Formation; Table S1) for stable isotope analysis. The  
316 selected examples showed no obvious signs of recrystallisation, fracture-filling cement or gley mottling (Fig.  
317 6). Profiles showing such features were deliberately avoided as the initial intention was to attempt direct  
318 calculation of Siluro-Devonian palaeoatmospheric  $p\text{CO}_2$  from calcrete  $\delta^{13}\text{C}$  (Cerling 1984; 1991; 1992; see  
319 below) and  $\delta^{13}\text{C}$  of fossil plants from the same locality. Gley mottling can indicate that the soil was  
320 waterlogged; rendering it unsuitable for use in the palaeosol  $p\text{CO}_2$  model, and recrystallisation can allow re-  
321 setting of the carbonate  $\delta^{13}\text{C}$  and  $\delta^{18}\text{O}$  compositions (Quast *et al.* 2006).

322

323 In thin-section the nodules are petrographically similar and typical of calcretes, exhibiting sharp to slightly  
324 diffuse boundaries, and surrounded by circumgranular cracks. Several of the nodules are composite,  
325 comprised of spar-cemented coalesced micritic peloids. Floating sand grains are rare but are encountered,  
326 commonly exhibiting corroded margins. The observed textures are compatible with a primary calcrete origin.

327

#### 328 *Ridgeway Conglomerate Formation palaeosols*

329 The Ridgeway Conglomerate Formation at Freshwater West (Fig. 1) comprises alluvial fan conglomerates  
330 interfingering with sheet sandstones, inclined and planar-laminated heterolithics and mudstones, interpreted as  
331 a low gradient fluvial system (Hillier & Williams 2007). Pedified mudstones are interpreted as calcic palaeo-  
332 Vertisols (Fig. 7a). They possess characteristic A horizons that are desiccation-cracked and calcretised, with  
333 drab-haloed root traces. These root traces may have originated from vascular plants, but fungal rooting  
334 structures have also been reported from this formation (Hillier *et al.* 2008). Some of the calcretes in this  
335 formation are of likely groundwater origin (Fig. 7b; Hillier *et al.* 2011a). These can be identified where they  
336 form thin continuous layers with sharp bases and tops.

337

338 Pedogenic calcretes are developed up to Stage III of Machette (1985), and rarely calcrete nodules are as large  
339 as 20 cm diameter. Some nodules are cross-cut by discontinuous and irregular sub-horizontal calcite-filled

340 cracks that are interpreted as pedogenic crystallaria (Fig. 7a). Such calcite-filled fractures typically form  
341 sheets sub-parallel to bedding (Hillier & Williams 2007). In thin-section, the more common smaller nodules  
342 comprise millimetre-sized dark micritic (pedogenic) peloids coated in c. 100 micron-thick layers of  
343 (phreatic?) calcitic microspar (Fig. 7c) that also infills millimetre-sized cavities (Fig. 7d). This microspar is  
344 consistent with a 'secondary' phreatic cement-precipitating phase that followed initial precipitation of dark  
345 micritic carbonate within the soil. However, the precipitation of the spar could have occurred within swampy,  
346 waterlogged soils at times of high water table, making it arguably 'syn-depositional'. The largest nodules  
347 from the top of the Ridgeway Conglomerate Formation at Freshwater West (ATB 220810-13; Table S1) are  
348 spherulitic, composed of curved columnar calcite crystals that grew out from a reduction spot in the nodule  
349 centre (Fig. 7e). The curving of the crystals can be ascribed to spherulitic crystal growth.

350

### 351 **Results of stable isotope geochemistry**

352

353 Bulk micritic samples of the nodules were micro-drilled for stable isotope analyses. Carbon and oxygen  
354 isotope data from this study (all VPDB) are tabulated in full in the supplementary information and presented  
355 here in a cross-plot (Fig. 8), and on a plot of collated Palaeozoic calccrete carbon isotope data (Fig. 9). A  
356 summary of the results is given in Table 1. Overall, calccrete carbon isotope values range from ca. -12‰  
357 (Conigar Pit Sandstone Member at Manorbier) to -6.9‰ (from near the top of the Ridgeway Conglomerate  
358 Formation at Freshwater West). Oxygen isotopes were mostly lower than -9‰, ranging from ca. -14‰ (from  
359 near the top of the Ridgeway Conglomerate Formation at Freshwater West) to -5.8‰ (from crystallaria in the  
360 Conigar Pit Sandstone Member at Freshwater West). A micro-milled thin-section of Conigar Pit Sandstone  
361 Member calccrete (Fig. 5a) yielded uniform  $\delta^{13}\text{C}$  values for central void-filling spar (-10.0‰), microsparry  
362 crystallaria around the void-filling spar (-10.1‰), and micritic nodule calcite (-10.1‰). The  $\delta^{18}\text{O}$  values of  
363 these samples showed some variation, with the latest-stage void-filling spar yielding a value of -8.1‰, the  
364 surrounding microsparry crystallaria -13.6‰, and the micritic nodule -13.8‰.

365

366 Two samples of coalified remains from rhyniophytoids from Tredomen Quarry (Morris *et al.* 2011) gave  $\delta^{13}\text{C}$   
367 of -24.2‰ and -25.0‰. Two samples of charcoaled *Prototaxites* gave  $\delta^{13}\text{C}$  of -24.6‰ and -25.5‰. One  
368 sample of coalified *Prototaxites* gave  $\delta^{13}\text{C}$  of -26.9‰ VPDB. These are all consistent with a primary origin  
369 from photosynthesising organisms using the  $\text{C}_3$  photosystem pathway. It is possible that the isotopic values

370 from *Prototaxites* reflect its heterotrophic consumption of C<sub>3</sub> photosynthesising organisms, rather than  
371 indicating *Prototaxites* was an autotrophic organism itself (e.g. Boyce *et al.* 2007).

372

## 373 **Discussion**

374

### 375 *Diagenesis and geochemical alteration of the oxygen isotopes*

376 Thin-sections of the pedogenic nodules reveal micritic peloids with circumgranular cracks that are interpreted  
377 as original soil textures (e.g. Fig. 5a; Table S1). Several of the features observed are consistent with  
378 precipitation of the micritic and microsparitic fabrics in waterlogged soils, including gleying and the circum-  
379 granular cracks themselves. Coarse, clear calcite spar and very minor vein-filling dolomite or siderite (the  
380 latter seen only in one late-stage spar-filling fracture) could conceivably reflect cementation of void spaces  
381 during burial. This ‘late stage’ calcite spar is found in burrows that were clearly syn-sedimentary voids  
382 (perhaps after organic matter oxidation) and circum-granular cracks that could have progressively opened as  
383 the water-logged soils dried out. Oxygen isotope values of c. -9 to -14‰ values seem incompatible with  
384 precipitation from meteoric waters in the interpreted sub-equatorial setting of these rocks in the Late Silurian  
385 and Early Devonian (Channell *et al.* 1992). They would, however, be consistent with re-setting of carbonate  
386  $\delta^{18}\text{O}$  by high temperature fluids during burial. One might speculate that the late-stage spar of the Conigar Pit  
387 Sandstone Member exhibits less negative  $\delta^{18}\text{O}$  and  $\delta^{13}\text{C}$  values than the relatively older micritic nodules and  
388 void-lining microsparitic crystallaria (Fig 5a and Fig. 8) because the spar was less susceptible to oxygen  
389 isotopic alteration than the micrite. Based on examination of Oligocene terrestrial carbonates of the  
390 Himalayas, however, Bera *et al.* (2010) considered that oxygen isotope compositions were best preserved in  
391 samples with over 70% micrite. They suggested that this was because the lowest water:rock ratios would  
392 normally be found in the most micritic samples. In the Conigar Pit Sandstone Member it seems possible the  
393 micrite was more permeable to oxygen isotope altering fluids than the spar.

394

### 395 *Post-depositional alteration of carbon isotopes?*

396

397 Carbonate carbon isotopes are less likely to be re-set than carbonate oxygen isotopes during burial because of  
398 a strong buffering effect from pre-existing carbonate carbon (e.g. Banner & Hanson 1990). The lack of  $\delta^{13}\text{C}$   
399 variation encountered between the three micromilled Conigar Pit Sandstone Member fabrics (early micrite,

400 early microspar, and late spar) can be interpreted as early-formed calcrete carbon dominating the  $\delta^{13}\text{C}$  signal  
401 of late-stage fluids, or alternatively complete late-stage overprinting of an earlier (higher)  $\delta^{13}\text{C}$  signal.

402

403 Rocks of the Anglo-Welsh Basin have experienced low grade metamorphism at temperatures of c.175 to  
404 350°C (up to lower greenschist facies; Bevins and Robinson, 1988). One consequence of low-temperature  
405 metamorphism of carbonates in the presence of silicates can be production and loss of  $\text{CO}_2$  ('decarbonation')  
406 such that carbon and oxygen stable isotopes may be affected. The carbon dioxide produced by such reactions  
407 is usually enriched in  $^{13}\text{C}$  and  $^{18}\text{O}$  in comparison to the calcite (Shieh and Taylor, 1969), meaning the calcite is  
408 likely to become relatively depleted in  $^{13}\text{C}$  and  $^{18}\text{O}$ . In addition, metasomatic fluids passing through the  
409 carbonate rock provide an opportunity for isotopic exchange to occur, particularly for oxygen. Rocks with a  
410 significant silicate component are liable to have experienced shifts in their oxygen and carbon stable isotopic  
411 compositions as a result of metamorphism, and these calcretes clearly fall in that category. However, large  
412 shifts in  $\delta^{13}\text{C}$  and  $\delta^{18}\text{O}$  (ca. 5 to 10 *per mil* decreases) by decarbonation only occur if substantial proportions  
413 of the carbon and oxygen are converted to  $\text{CO}_2$  and lost from the rock (Valley, 1986). Large effects are  
414 usually found in cases of contact metamorphism that also include a component of equilibration of isotopically  
415 light igneous  $\text{CO}_2$  with sedimentary carbonate  $\text{CO}_2$  (see Valley, 1986). In the Old Red Sandstone strata  
416 examined, the lack of minerals that are common products of decarbonation reactions (e.g. wollastonite and  
417 tremolite) and lack of evidence for substantial recrystallisation of the calcretes, argues against significant  
418 metamorphic effects on their carbon and oxygen isotope values.

419

420 A negative shift in calcrete  $\delta^{13}\text{C}$  could result from post-depositional isotopic exchange with a significant  
421 external source of organic carbon. However there is no clear evidence of carbon migration (such as veining)  
422 from underlying Ordovician organic-rich shales into the Old Red Sandstone sections investigated. The carbon  
423 isotopic compositions of marine carbonates of the Coralliferous Formation (which lies stratigraphically  
424 between the Ordovician shales and the lower Old Red Sandstone units described here) were measured to  
425 determine whether they have been affected by migration of organic carbon from Ordovician shales. These  
426 limestones gave bulk compositions in the region of ca. -2‰ VPDB (our unpublished data), suggesting there  
427 has not been a significant upward migration of low  $\delta^{13}\text{C}$  carbon into the Coralliferous Formation (and, by  
428 inference, the overlying Old Red Sandstone units). It is concluded that the most likely source of isotopically  
429 light carbon that could have affected the carbon isotopic compositions of these nodules during deep burial is  
430 organic matter from within the ancient soils themselves.

431

432 The strongest evidence against significant post-depositional re-setting of these calcrete carbon isotopic signals  
433 comes from their unaltered petrographic appearances, which are hard to reconcile with geochemical processes  
434 that would demand substantial recrystallization sufficient to affect the carbon signals. Field and petrographic  
435 evidence (including, for example, nodules reworked in conglomerates) suggests most of the calcite  
436 precipitation occurred prior to burial, and the geochemical data do not require input of carbon from any source  
437 other than organic matter originally present in the (likely seasonally waterlogged) soils.

438

#### 439 *Explanations for low calcrete $\delta^{13}\text{C}$ values*

440 Assuming that the carbon isotopic compositions of these calcretes are mostly unaltered then consideration  
441 must be given to why these values are more negative than those of North American calcretes of similar age  
442 (see Fig. 9). One explanation might be that calcrete precipitation took place under different conditions. Mora  
443 *et al.* (1991) and Driese *et al.* (1992) suggested that the precipitation of the North American Bloomsburg  
444 Formation calcretes took place at shallow soil depths (a few centimetres), given small Silurian plant rooting  
445 systems (e.g. Algeo *et al.* 1995). In the Bloomsburg Formation palaeosols, this would have favoured a strong,  
446 relatively  $^{13}\text{C}$  rich atmospheric  $\text{CO}_2$  contribution to the calcrete  $\delta^{13}\text{C}$  (e.g. Mora *et al.* 1996), resulting in  
447 isotopic values of  $> -7\text{‰}$  (Driese *et al.* 1992). Perhaps the contribution of atmospheric  $\text{CO}_2$  to the Old Red  
448 Sandstone calcretes was relatively lower than found in the North American examples. This could be the case  
449 if the Old Red Sandstone soils originally contained greater volumes of respiring organisms and oxidizing  
450 organic matter. Determining the relative contributions of organic matter from these two settings is challenging  
451 because the majority of the plant material has not been preserved. No plant fossils were described in  
452 association with the Bloomsburg paleosols (Driese *et al.*, 1992). However, in general the plant fossil record  
453 from the Bloomsburg Formation is meager, the most significant report from Ludlovian strata being non-  
454 vascular thalloid fragments that are part of the *Nematothallus* complex (Strother, 1988). In comparison the  
455 plant assemblages from the latest Silurian to earliest Devonian Anglo-Welsh Basin are more abundant and  
456 diverse, with evidence of vascular plants (Edwards and Richardson, 2004). It is notable that Lower  
457 Cretaceous calcretes of the Wealden Beds, UK, that were also deposited in partially waterlogged to marshy  
458 soils, have very comparable  $\delta^{13}\text{C}$  values ( $-9$  to  $-12.5\text{‰}$ ; Robinson *et al.*, 2002). There, Robinson *et al.* (2012)  
459 suggested the ingress of atmospheric  $\text{CO}_2$  to the soils was low to negligible. In these scenarios of soils  
460 inhabited by abundant plants the Old Red Sandstone calcrete carbon isotope signals would be dominated by  
461 isotopically light carbon from the organic matter.

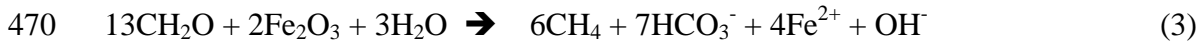
462

463 Further possibilities might include the effects of soil zone microbiota. First, in anoxic environments anaerobic  
464 methanogenesis can provide a source of dissolved carbon that has extremely low  $\delta^{13}\text{C}$  values (commonly ca. -  
465 75‰; Irwin et al., 1977; Whiticar, 1999):



467

468 Due to production of  $\text{CO}_2$ , an accompanying lowering of soil water pH is expected, unless methanogenesis is  
469 coupled to significant Fe(III) reduction (Andrews et al., 1991):



471

472 However such methanogenesis usually occurs in environments lacking acetate (Whiticar, 1999). These places  
473 are mostly proximate to areas that are sulphate-rich, where sulphate reducing bacteria can out compete  
474 methanogens for the acetate (Whiticar, 1999). Sulphate minerals (or their pseudomorphs) and sulphides are  
475 distinctly lacking in the examined sections, so the above mechanisms can probably be discounted.

476

477 Where acetate ( $\text{CH}_3\text{COO}^-$ ) is present (i.e. where bacterial sulphate reduction is not prevalent), methanogenesis  
478 can occur through acetate fermentation:



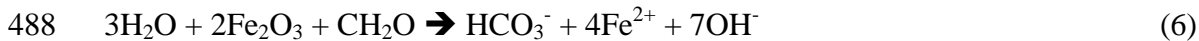
480

481 Subsequent oxidation of the methane by iron reduction could supply very low  $\delta^{13}\text{C}$  dissolved carbon  
482 (Andrews et al., 1991):



484

485 There is clear evidence of iron reduction in the studied sections such as gley mottling, and even reduction  
486 spots in some nodule centres. Such features could also have been produced by anaerobic microbial oxidation  
487 of organic matter, using  $\text{Fe}^{3+}$  as the oxidant (Andrews et al., 1991):



489

490 The  $\delta^{13}\text{C}$  of the bicarbonate produced via organic matter oxidation would reflect the  $\delta^{13}\text{C}$  of the organic  
491 matter (measured here as -25‰). Direct oxidation of the organic matter (i.e., aerobic respiration by soil zone



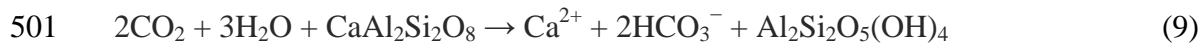
492 organisms including plant roots, fungi and invertebrates), or of biogenic methane, could obviously also occur  
493 in oxic conditions (e.g. Irwin et al., 1977):

494



497

498 Here some carbonic acid is produced that could be used in the chemical weathering of pre-existing carbonate  
499 rock, or more likely in this case of calcium silicate grains from interbedded volcanic ash horizons (e.g. Berner,  
500 1992; reaction 9):



502

503 Through supply of calcium ions, reaction 9 could help to drive calcite precipitation (via reaction 1). A likely  
504 product of this chemical weathering is kaolinite, which has been found in Lower Old Red Sandstone rocks of  
505 Wales (Hillier et al., 2006). Some of this kaolinite has been interpreted as potentially having survived  
506 diagenesis (Hillier et al., 2006), while illite, the likely product of kaolinite diagenesis, is common in the clays  
507 of Freshwater West (Hillier et al., 2006).

508

509 A key feature of all of the above processes is that they require the presence of organic matter, or at least of  
510 organic carbon compounds derived from breakdown of such material, within the ancient soils. Reactions 4, 5  
511 and 6 all take place in anoxic conditions (including waterlogged soils) and have the advantage of directly  
512 explaining features associated with iron reduction. Yet the calcretes examined are non-ferroan to only slightly  
513 ferroan, staining dominantly pink to rarely purple with Alizarin Red S and potassium ferricyanide. This  
514 suggests they dominantly formed under oxic conditions, with low  $\delta^{13}\text{C}$  carbon liberated via oxidation of  
515 organic matter following reactions 7 and 8. Calcrete formation under oxic conditions is clearly also  
516 compatible with the red colouration of these clay-rich Old Red Sandstone rocks.

517

518 The strong and consistent signal from  $\text{C}_3$  photosynthesis seen in the  $\delta^{13}\text{C}$  of the calcretes measured, together  
519 with the  $\delta^{13}\text{C}$  of organic matter, the lack of sulphides or sulphates, and the great abundance of carbonate  
520 nodules, is taken as evidence for significant organic matter oxidation in (and later de-gassing of  $\text{CO}_2$  from)  
521 these ancient soils. The palaeoclimate must have been strongly seasonal. During the wet season, plant-  
522 associated respiration in the soils was high. When soils were waterlogged anaerobic microbial oxidation of

523 organic matter (plus some methanogenesis) may have occurred. These processes will have generated carbonic  
524 acid, which in turn liberates calcium ions. Most calcrete precipitation likely took place during the dry season,  
525 as evapotranspiration increased concentrations of calcium ions in increasingly oxic soil waters, and CO<sub>2</sub> de-  
526 gassed to the atmosphere. Because carbonic acid-rich soils enhance chemical weathering of silicate bedrock,  
527 implicated in drawdown of atmospheric CO<sub>2</sub> levels (e.g. Berner 1998), this finding is of relevance to  
528 modelling Silurian to Devonian atmospheric pCO<sub>2</sub> (e.g. Lenton *et al.* 2012).

529

### 530 *Calculation of palaeoatmospheric CO<sub>2</sub>*

531 In the right circumstances palaeoatmospheric CO<sub>2</sub> concentrations can be directly estimated from pedogenic  
532 calcrete δ<sup>13</sup>C (e.g. Cerling 1984, 1991, 1992; Driese *et al.* 1992; Andrews *et al.* 1995; Ekart *et al.* 1999; Royer  
533 *et al.* 2001; Breecker *et al.* 2010; Bera *et al.* 2010). This is because a high (palaeo-)atmospheric CO<sub>2</sub>  
534 contribution to soil zone gases can result in <sup>13</sup>C-rich calcretes, while high contributions from respired CO<sub>2</sub>  
535 (including oxidation of isotopically light vegetation) drive δ<sup>13</sup>C of pedogenic calcrete to lower values. The  
536 equation for estimating palaeoatmospheric pCO<sub>2</sub> from calcrete δ<sup>13</sup>C (after Cerling 1984; 1991; Ekart *et al.*  
537 1999) is:

538

$$539 C_{\text{air}} = S(z) * (\delta^{13}\text{C}_s - 1.0044 \delta^{13}\text{C}_\phi - 4.4 / \delta^{13}\text{C}_{\text{air}} - \delta^{13}\text{C}_s) \quad (3)$$

540

541 where C<sub>air</sub> is the calculated CO<sub>2</sub> concentration of the palaeoatmosphere; S(z) is the CO<sub>2</sub> contribution from soil  
542 respiration as a function of depth (z); δ<sup>13</sup>C<sub>s</sub> is the δ<sup>13</sup>C of soil CO<sub>2</sub> (calculated from calcrete δ<sup>13</sup>C using the  
543 temperature dependent fractionation factor of Romanek *et al.* 1992); δ<sup>13</sup>C<sub>φ</sub> is the δ<sup>13</sup>C of soil respired CO<sub>2</sub>  
544 (measured from contemporaneous organic carbon); and δ<sup>13</sup>C<sub>air</sub> is the δ<sup>13</sup>C of palaeoatmospheric CO<sub>2</sub> (here  
545 calculated from δ<sup>13</sup>C<sub>org</sub> of -25‰, assuming consistent fractionation by photosynthesis, to be -5.75‰, using  
546 Schaller *et al.*, 2011). On the basis of calcrete δ<sup>13</sup>C values around -5‰ from the Silurian Bloomsburg  
547 Formation of North America, Mora *et al.* (1991) and Driese *et al.* (1992) concluded that Silurian to Early  
548 Devonian atmospheric pCO<sub>2</sub> was very high: above 3000 ppmV.

549

550 In the case of the Siluro-Devonian soil carbonates described here, it is not clear that they are a suitable source  
551 for deducing palaeoatmospheric pCO<sub>2</sub>. Firstly, it is recommended that calcrete samples are taken from at least  
552 50cm depth below the palaeosurface (Royer *et al.*, 2001). This is because in modern soils of the south western  
553 USA, soil carbonate δ<sup>13</sup>C has been shown to be variable above this depth due to mixing of soil respired CO<sub>2</sub>

554 and atmospheric CO<sub>2</sub> (Cerling, 1984; Ekart et al., 1999). In common with most palaeosols, it is not easy to tell  
555 whether many of the nodules described here originally formed at 50cm depth or less. This is in part because of  
556 syn-depositional movement via the self-mulching process (argillopedoturbation), as well as truncation of the  
557 A horizons (Marriott & Wright 2006). Secondly, there is considerable uncertainty over the correct value to  
558 use for S(z). An exceptionally high value of 20 000 ppmV (Royer *et al.* 2001) might be appropriate if the soils  
559 were waterlogged when most of the carbonate precipitated. In their study of Lower Cretaceous calcretes  
560 formed in seasonally waterlogged soils, Robinson et al. (2002) chose to apply an S(z) value of 10 000 ppmV.  
561 However this S(z) value was too low to allow palaeoatmospheric pCO<sub>2</sub> calculation from calcretes inferred to  
562 have formed in the wettest, marshy palaeoenvironments. Third, using a value for  $\delta^{13}\text{C}\phi$  obtained from  
563 measurement of contemporaneous organic carbon (-25‰) ignores the possibility here of a methanogenic  
564 contribution to soil respired CO<sub>2</sub>. Using a lower value for  $\delta^{13}\text{C}\phi$ , allowing for some methanogenesis  
565 would raise the calculated palaeoatmospheric pCO<sub>2</sub>.

566  
567 If unaltered, our carbon isotope data would only be broadly compatible with the high Late Silurian  
568 atmospheric pCO<sub>2</sub> that Mora *et al.* (1991) and Driese *et al.* (1992) suggest if a very high value for S(z)  
569 applies, or if  $\delta^{13}\text{C}\phi$  was lower than -25‰. For example, using our measured organic carbon  $\delta^{13}\text{C}$  value of -  
570 25‰ with a micritic calcrete  $\delta^{13}\text{C}$  value of -10.1‰ (Conigar Pit Sandstone Member micromilled sample) at  
571 25 °C with an S(z) value of 20 000 ppmV yields a calculated palaeoatmospheric pCO<sub>2</sub> of c. 2500 ppmV.  
572 However, Breecker et al., 2010, noted that most modern calcrete precipitation in semi-arid environments  
573 occurs during dry seasons, when values of S(z) are significantly lower (c. 2500 ppmV). Using an S(z) value of  
574 2500 ppmV, with all other parameters as above, yields a calculated palaeoatmospheric pCO<sub>2</sub> of just 300  
575 ppmV. Further constraints on the correct value to use for S(z) here, and on  $\delta^{13}\text{C}\phi$ , are therefore required  
576 before reliable estimates of palaeoatmospheric pCO<sub>2</sub> can be made from these palaeosol carbonates.

## 578 **Conclusions**

579 The Moor Cliffs Formation, Freshwater West Formation and Ridgeway Conglomerate Formation all have  
580 calcrete  $\delta^{13}\text{C}$  values within the range of -7 to -12‰, with an average of -10.1‰ (VPDB). The most likely  
581 source of isotopically light carbon that could have exchanged with the carbonate carbon during burial is  
582 intraformational organic matter. The carbon isotopes suggest these widespread and abundant pedogenic  
583 calcrete nodules formed principally by de-gassing of CO<sub>2</sub> from seasonally water-logged, organic-carbon rich  
584 soils, to the atmosphere. If these assumptions are correct then calculations of Late Silurian atmospheric pCO<sub>2</sub>

585 from our calcrete carbon isotope data could only yield results broadly consistent with those obtained from  
586 North American soils of similar age (Mora *et al.* 1991; Driese *et al.* 1992) if an exceptionally high value of 20  
587 000 ppmV is used for S(z) in these calculations, or if our estimated value of -25‰ for  $\delta^{13}\text{C}\phi$  is too low.  
588 Relative lack of constraint on these parameters highlights a need for further research on ancient microbial  
589 processes in fossil soils.

590

### 591 **Acknowledgements**

592 This work was part-supported by a grant from the E J Garwood Fund (2011) of the Geological Society of  
593 London. Julie Dougans (SUERC) and Suzanne Verdegaal (VU Amsterdam) kindly assisted with some of the  
594 stable isotope measurements. Dineke Brasier kindly assisted with fieldwork. Work on Tredomen Quarry  
595 calcrete samples was conducted by JLM as part of a PhD funded by the School of Earth and Ocean Sciences,  
596 Cardiff University, under the supervision of Prof. V.P. Wright and Prof. D. Edwards. Core drilling was partly  
597 funded by the British Geological Survey. Thanks to Julia Becker (Cardiff University) for isotopic analysis of  
598 the Tredomen Quarry calcretes. Thanks to Geoff Abbott (Newcastle University) and Iso-Analytical Ltd for  
599 isotopic analysis of fossil plant material. Three anonymous reviewers and the editor made helpful suggestions  
600 that improved the quality of the manuscript.

601

### 602 **References**

- 603 ALGEO, T.J., BERNER, R.A., MAYNARD, J.B. & SCHECKLER, S.E. 1995. Late Devonian oceanic anoxic events  
604 and biotic crises: 'rooted' in the evolution of vascular land plants? *GSA Today*, **5**, 64-66.
- 605 ALGEO, T.J., SCHECKLER, S.E. & MAYNARD, J.B. 2001. Effects of the Middle to Late Devonian spread of  
606 vascular land plants on weathering regimes, marine biotas and global climate. *In*: GENSEL, P.G. &  
607 EDWARDS, D. (eds) *Plants Invade The Land: Evolutionary and Environmental Perspectives*. New  
608 York, Columbia University Press, 213-236.
- 609 ALLEN, J.R.L. 1974. Sedimentology of the Old Red Sandstone (Siluro-Devonian) in the Cleve Hills area,  
610 Shropshire, England. *Sedimentary Geology*, **12**, 73-167.
- 611 ALLEN, J.R.L. 1985. Marine to Fresh Water: The Sedimentology of the Interrupted Environmental Transition  
612 (Ludlow-Siegenian) in the Anglo-Welsh Region. *Philosophical Transactions of the Royal Society of*  
613 *London, Series B, Biological Sciences*, **309**, 85-104.

- 614 ALLEN, J.R.L. 1986. Pedogenic calcretes in the Old Red Sandstone facies (Late Silurian—Early  
615 Carboniferous) of the Anglo-Welsh area, southern Britain. *In: WRIGHT, V.P. (ed) Palaeosols: Their  
616 Recognition and Interpretation*. Oxford, U.K., Blackwell, 56-86.
- 617 ALLEN, J.R.L. & DINELEY, D. L. 1986. The succession of the Lower Old Red Sandstone (Siluro-Devonian)  
618 along the Ross-Tewkesbury Spur Motorway (M.50), Hereford and Worcester. *Geological Journal*, **11**,  
619 1-14.
- 620 ALLEN, J.R.L. & WILLIAMS, B.P.J. 1979. Interfluvial drainage on Siluro-Devonian alluvial plains in Wales  
621 and the Welsh Borders. *Journal of the Geological Society*, **136**, 361-366.
- 622 ALLEN, J.R.L. & WILLIAMS, B.P.J. 1981. Sedimentology and stratigraphy of the Townsend Tuff Bed (Lower  
623 Old Red Sandstone) in South Wales and the Welsh Borders. *Journal of the Geological Society*, **138**,  
624 15-29.
- 625 ALLEN, J.R.L. & WILLIAMS, B.P.J. 1982. The architecture of an alluvial suite: rocks between the Townsend  
626 Tuff and Pickard Bay Tuff Beds (Early Devonian), Southwest Wales. *Philosophical Transactions of  
627 the Royal Society of London Series B*, **287**, 51-89.
- 628 ANDREWS, J.E., TURNER, M.S., NABI, G. & SPIRO, B. 1991. The anatomy of an early Dinantian terraced  
629 floodplain: palaeo-environment and early diagenesis. *Sedimentology*, **38**, 271-287.
- 630 ANDREWS, J.E., TANDON, S.K. & DENNIS, P.F. 1995. Concentration of carbon in the Late Cretaceous  
631 atmosphere. *Journal of the Geological Society*, **152**, 1-3.
- 632 BANNER, J.L. & HANSON, G.N. 1990. Calculation of simultaneous isotopic and trace element variations  
633 during water-rock interaction with applications to carbonate diagenesis. *Geochimica et Cosmochimica  
634 Acta*, **54**, 3123-3137.
- 635 BARCLAY, W.J., BROWNE, M.A.E., MCMILLAN, A.A., PICKETT, E.A., STONE, P. & WILBY, P.R. 2005. *The Old  
636 Red Sandstone of Great Britain*. Geological Conservation Review Series, No. 31, Joint Nature  
637 Conservation Committee, Peterborough.
- 638 BARCLAY, W. J., DAVIES, J.R., HILLIER, R.D. and WATERS, R.A. in press. Lithostratigraphy of the Old Red  
639 Sandstone successions of the Anglo-Welsh Basin. *British Geological Survey Research Report*,  
640 RR/11/00.
- 641 BERA, M.K., SARKAR, A., TANDON, S.K., SAMANTA, A. & SANYAL, P. 2010. Does burial diagenesis reset  
642 pristine isotopic compositions in paleosol carbonates? *Earth and Planetary Science Letters*, **300**, 85-  
643 100.

644 BERNER, R.A. 1998. The carbon cycle and carbon dioxide over Phanerozoic time: the role of land plants.  
645 *Philosophical Transactions of the Royal Society of London. Series B: Biological Sciences*, **353**, 75-82.

646 BERNER, R.A. & KOTHAVALA, Z. 2001. Geocarb III: A revised model of atmospheric CO<sub>2</sub> over Phanerozoic  
647 time. *American Journal of Science*, **301**, 182-204.

648 BERNER, E.K., BERNER, R.A. & MOULTON, K.L. 2003. Plants and Mineral Weathering: Present and Past. *In*:  
649 Holland, H.D. & TUREKIAN, K.K. (eds) *Treatise on Geochemistry*. Oxford, Pergamon, **5**, 169-188.

650 BEVINS, R.E. & ROBINSON, D. 1988. Low grade metamorphism of the Welsh Basin Lower Palaeozoic  
651 succession: an example of diastothermal metamorphism? *Journal of the Geological Society of London*,  
652 **145**, 363-366.

653 BOYCE, C.K., HOTTON, C.L., FOGEL, M.L., CODY, G.D., HAZEN, R.M., KNOLL, A.H. & HUEBER, F.M. 2007.  
654 Devonian landscape heterogeneity recorded by a giant fungus. *Geology*, **35**, 399-402.

655 BRASIER, A.T. 2011. Searching for travertines, calcretes and speleothems in deep time: Processes,  
656 appearances, predictions and the impact of plants. *Earth-Science Reviews*, **104**, 213-239.

657 BREECKER, D.O., SHARP, Z.D. & MCFADDEN, L.D. 2010. Atmospheric CO<sub>2</sub> concentrations during ancient  
658 greenhouse climates were similar to those predicted for A.D. 2100. *Proceedings of the National  
659 Academy of Sciences*, **107**, 576-580.

660 BUGGISCH, W., KELLER, M. & LEHNERT, O. 2003. Carbon isotope record of Late Cambrian to Early  
661 Ordovician carbonates of the Argentine Precordillera. *Palaeogeography, Palaeoclimatology,  
662 Palaeoecology*, **195**, 357-373.

663 CAPO, R.C., CHADWICK, O.A. 1999. Sources of strontium and calcium in desert soil and calcrete. *Earth and  
664 Planetary Science Letters*, **170**, 61-72.

665 CERLING, T.E. 1984. The stable isotopic composition of modern soil carbonate and its relationship to climate.  
666 *Earth and Planetary Science Letters*, **71**, 229-240.

667 CERLING, T.E. 1991. Carbon dioxide in the atmosphere: evidence from Cenozoic and Mesozoic paleosols.  
668 *American Journal of Science*, **291**, 377-400.

669 CERLING, T.E. 1992. Further comments on using carbon isotopes in palaeosols to estimate the CO<sub>2</sub> content of  
670 the palaeo-atmosphere. *Journal of the Geological Society*, **149**, 673-676.

671 CHANNELL, J.E.T., MCCABE, C., TORSVIK, T.H., TRENCH, A. & WOODCOCK, N.H. 1992. Palaeozoic  
672 palaeomagnetic studies in the Welsh Basin - recent advances. *Geological Magazine*, **129**, 533-542.

- 673 DE ROS, L.F., MORAD, S. & PAIM, P.S.G. 1994. The role of detrital composition and climate on the diagenetic  
674 evolution of continental molasses: evidence from the Cambro--Ordovician Guaritas Sequence,  
675 southern Brazil. *Sedimentary Geology*, **92**, 197-228.
- 676 DRIESE, S.G. & MORA, C.I. 1993. Physico-chemical environment of pedogenic carbonate formation in  
677 Devonian vertic paleosols, central Appalachians, USA. *Sedimentology*, **40**, 199-216.
- 678 DRIESE, S.G., MORA, C.I., COTTER, E. & FOREMAN, J.L. 1992. Paleopedology and stable isotope  
679 geochemistry of Late Silurian vertic paleosols, Bloomsburg Formation, central Pennsylvania. *Journal*  
680 *of Sedimentary Petrology*, **62**, 825-841.
- 681 EDWARDS, D. 1979. A Late Silurian flora from the Lower Old Red Sandstone of south-west Dyfed.  
682 *Palaeontology*, **22**, 23-52.
- 683 EDWARDS, D. & RICHARDSON, J.B. 2004. Silurian and Lower Devonian plant assemblages from the Anglo-  
684 Welsh Basin: a palaeobotanical and palynological synthesis. *Geological Journal*, **39**, 375-402.
- 685 EKART, D.D., CERLING, T.E., MONTAÑEZ, I.P. & TABOR, N.J. 1999. A 400 million year carbon isotope record  
686 of pedogenic carbonate: implications for paleoatmospheric carbon dioxide. *American Journal of*  
687 *Science*, **299**, 805-827.
- 688 FRIEND, P.F., WILLIAMS, B.P.J., FORD, M., & WILLIAMS, E.A. 2000. Kinematics and dynamics of Old Red  
689 Sandstone basins. In: FRIEND, P.F. & WILLIAMS, B.P.J. (eds) *New Perspectives on the Old Red*  
690 *Sandstone*. Geological Society, London, Special Publications **339**, 29-60.
- 691 GOUDIE, A. 1973. *Duricrust in tropical and subtropical landscapes*. Clarendon Press, Oxford, 174p.
- 692 HIGGS, K.T. 2004. An Early Devonian (Lochkovian) microflora from the Freshwater West Formation, Lower  
693 Old Red Sandstone, southwest Wales. *Geological Journal*, **39**, 359-374.
- 694 HILLIER, R.D. & WILLIAMS, B.P.J. 2006. The alluvial Old Red Sandstone: fluvial basins. In: BRENCHLEY, P.J.  
695 & RAWSON, P.F. (eds) *The Geology of England and Wales, Second Edition*. Geological Society of  
696 London. Bath, 155-172.
- 697 HILLIER, R.D. & WILLIAMS, B.P.J. 2007. The Ridgeway Conglomerate Formation of SW Wales, and its  
698 implications. The end of the Lower Old Red Sandstone? *Geological Journal*, **42**, 55-83.
- 699 HILLIER, R.D., MARRIOTT, S.B., WILLIAMS, B.P.J. & WRIGHT, V.P. 2007. Possible climate variability in the  
700 Lower Old Red Sandstone Conigar Pit Sandstone Member (Early Devonian), South Wales, UK.  
701 *Sedimentary Geology*, **202**, 35-57.

702 HILLIER, R.D., EDWARDS, D. & MORRISSEY, L.B. 2008. Sedimentological evidence for rooting structures in  
703 the Early Devonian Anglo-Welsh Basin (UK), with speculation on their producers. *Palaeogeography,*  
704 *Palaeoclimatology, Palaeoecology*, **270**, 366-380.

705 HILLIER, R.D., MARRIOTT, S.B. & WILLIAMS, B.P.J. 2011a. Pedogenic and non-pedogenic calcretes in the  
706 Devonian Ridgeway Conglomerate Formation of SW Wales, UK: a cautionary tale. In: NORTH, C.P.,  
707 LELEU, S. & DAVIDSON, S. (eds) *From River To Rock Record: The Preservation Of Fluvial Sediments*  
708 *And Their Subsequent Interpretation*. Society of Economic Paleontologists and Mineralogists Special  
709 Publications, **97**, 311-325.

710 HILLIER, R.D., WATERS, R.A., MARRIOTT, S.B. & DAVIES, J.R. 2011b. Alluvial fan and wetland interactions:  
711 evidence of seasonal slope wetlands from the Silurian of south central Wales, UK. *Sedimentology*, **58**,  
712 831-853.

713 HILLIER, S., WILSON, M.J. & MERRIMAN, R.J. 2006. Clay mineralogy of the Old Red Sandstone and Devonian  
714 sedimentary rocks of Wales, Scotland and England. *Clay Minerals*, **41**, 433-471.

715 IRWIN, H., CURTIS, C. & COLEMAN, M. 1977. Isotopic evidence for source of diagenetic carbonates formed  
716 during burial of organic-rich sediments. *Nature*, **269**, 209-213.

717 JENKINS, G. 1998. *An investigation of marine influence during deposition of the Lower Old Red Sandstone,*  
718 *Anglo-Welsh Basin, UK*: University of Wales, Cardiff, Cardiff.

719 KAUFMAN, A.J. & KNOLL, A.H. 1995. Neoproterozoic variations in the C-isotopic composition of seawater:  
720 stratigraphic and biogeochemical implications. *Precambrian Research*, **73**, 27-49.

721 KELLER, C.K. & WOOD, B.D. 1993. Possibility of chemical weathering before the advent of vascular land  
722 plants. *Nature*, **364**, 223-225.

723 KELLER, M., BUGGISCH, W. & BERCOWSKI, F. 1989. Facies and sedimentology of Upper Cambrian  
724 shallowing-upward cycles in the La Flecha Formation (Argentine Precordillera). *Zentralblatt für*  
725 *Geologie und Paläontologie, Teil I*, 999-1011.

726 LAMPLUGH, G.W. 1902. Calcrete. *Geological Magazine*, **9**, 75.

727 LANG, W.H. 1937. On the plant-remains from the Downtonian of England and Wales. *Philosophical*  
728 *Transactions of the Royal Society B: Biological Sciences*, **227**, 245-291.

729 LENTON, T.M., CROUCH, M., JOHNSON, M., PIRES, N. & DOLAN, L. 2012. First plants cooled the Ordovician.  
730 *Nature Geoscience*, **5**, 86-89.



- 731 LOVE, S.E. & WILLIAMS, B.P.J. 2000. Sedimentology, cyclicity and floodplain architecture in the Lower Old  
732 Red Sandstone of SW Wales. *In: FRIEND, P.F. & WILLIAMS, B.P.J. (eds) New Perspectives on the Old*  
733 *Red Sandstone*. London, Geological Society of London, **180**, 371-388.
- 734 MACHETTE, M.N. 1985. Calcic soils of the southwestern United States. *Geological Society of America Special*  
735 *Paper*, **203**, 1-21.
- 736 MARRIOTT, S.B. & WRIGHT, V.P. 1993. Palaeosols as indicators of geomorphic stability in two Old Red  
737 Sandstone alluvial suites, South Wales. *Journal of the Geological Society*, **150**, 1109-1120.
- 738 MARRIOTT, S.B. & WRIGHT, V.P. 1996. Sediment recycling on Siluro–Devonian floodplains. *Journal of the*  
739 *Geological Society, London*, **153**, 661–664.
- 740 MARRIOTT, S.B. & WRIGHT, V.P. 2004. Mudrock deposition in an ancient dryland system: Moor Cliffs  
741 Formation, Lower Old Red Sandstone, southwest Wales, UK. *Geological Journal*, **39**, 277-298.
- 742 MARRIOTT, S.B. & WRIGHT, V.P. 2006. Investigating paleosol completeness and preservation in mid-  
743 Paleozoic alluvial paleosols: A case study in paleosol taphonomy from the Lower Old Red Sandstone.  
744 *In: ALONSO-ZARZA, A.M. & TANNER, L.H. (eds.) Palaeoenvironmental record and application of*  
745 *calcretes and palustrine carbonates*. Geological Society of America Special Paper 416, p43-52.
- 746 MARRIOTT, S.B., MORRISSEY, L.B. & HILLIER, R.D. 2009. Trace fossil assemblages in Upper Silurian tuff  
747 beds: Evidence of biodiversity in the Old Red Sandstone of southwest Wales, UK. *Palaeogeography,*  
748 *Palaeoclimatology, Palaeoecology*, **274**, 160-172.
- 749 MARRIOTT, S.B., HILLIER, R.D. & MORRISSEY, L.B. 2012. Enigmatic sedimentary structures in the Lower Old  
750 Red Sandstone, south Wales, UK: possible microbial influence on surface processes and early  
751 terrestrial food webs. *Geological Magazine*, **150** (3), 396-411.
- 752 MORA, C.I., DRIESE, S.G. & SEAGER, P.G. 1991. Carbon dioxide in the Paleozoic atmosphere: Evidence from  
753 carbon-isotope compositions of pedogenic carbonate. *Geology*, **19**, 1017-1020.
- 754 MORA, C.I., DRIESE, S.G. & COLARUSSO, L.A. 1996. Middle to Late Paleozoic atmospheric CO<sub>2</sub> levels from  
755 soil carbonate and organic matter. *Science*, **271**, 1105-1107.
- 756 MORRIS, J.L., RICHARDSON, J.B. & EDWARDS, D. 2011. Lower Devonian plant and spore assemblages from  
757 Lower Old Red Sandstone strata of Tredomen Quarry, South Wales. *Review of Palaeobotany and*  
758 *Palynology*, **165**, 183-208.
- 759 MORRIS, J.L., WRIGHT, V.P. & EDWARDS, D. 2012. Siluro-Devonian landscapes of southern Britain: the  
760 stability and nature of early vascular plant habitats. *Journal of the Geological Society, London*, **169**,  
761 173-190.

762 MORRISSEY, L.B., HILLIER, R.D. & MARRIOTT, S.B. 2012. Late Silurian and Early Devonian terrestrialisation:  
763 ichnological insights from the Lower Old Red Sandstone Anglo-Welsh Basin. *Palaeogeography,*  
764 *Palaeoclimatology, Palaeoecology*, **337-338**, 194-215.

765 QUAST, A., HOEFS, J. & PAUL, J. 2006. Pedogenic carbonates as a proxy for palaeo-CO<sub>2</sub> in the Palaeozoic  
766 atmosphere. *Palaeogeography, Palaeoclimatology, Palaeoecology*, **242**, 110-125.

767 ROBINSON, S.A., ANDREWS, J.E., HESSELBO, S.P., RADLEY, J.D., DENNIS, P.F., HARDING, I.C. & ALLEN, P.  
768 (2002) Atmospheric pCO<sub>2</sub> and depositional environments from stable-isotope geochemistry of  
769 calcrete nodules (Barremian, Lower Cretaceous, Wealden Beds, England). *Journal of the Geological*  
770 *Society of London*, **159**, 215-224.

771 ROMANEK, C.S., GROSSMAN, E.L. & MORSE, J.W. 1992. Carbon isotopic fractionation in synthetic aragonite  
772 and calcite: Effects of temperature and precipitation rate. *Geochimica et Cosmochimica Acta*, **56**, 419-  
773 430.

774 ROYER, D.L., BERNER, R.A. & BEERLING, D.J. 2001. Phanerozoic atmospheric CO<sub>2</sub> change: evaluating  
775 geochemical and paleobiological approaches. *Earth-Science Reviews*, **54**, 349-392.

776 SCHALLER, M.F., WRIGHT, J.D., & KENT, D.V. 2011. Atmospheric PCO<sub>2</sub> perturbations associated with the  
777 Central Magmatic Province. *Science*, **331**, 1404-1409.

778 SHIEH, Y.N. & TAYLOR, H.P. 1969. Oxygen and Carbon Isotope Studies of Contact Metamorphism of  
779 Carbonate Rocks. *Journal of Petrology*, **10**, 307-331.

780 SOIL SURVEY STAFF. 1999. *Soil taxonomy: A basic system of soil classification for making and interpreting*  
781 *soil surveys*. 2nd edition. Natural Resources Conservation Service. U.S. Department of Agriculture  
782 Handbook, pp. 436.

783 STROTHER, P.K., 1988. New species of *Nematothallus* from the Silurian Bloomsburg Formation of  
784 Pennsylvania. *Journal of Palaeontology*, **62**, 967-982.

785 VALLEY, J.W. 1986. Stable isotope geochemistry of metamorphic rocks. In: Valley, J.W., Taylor, H.P.,  
786 O'Neil, J.R. (eds.), *Stable Isotopes in High Temperature Geological Processes*. Reviews in  
787 Mineralogy. Mineralogical Society of America, 445-490.

788 VERRECCHIA, E.P., FREYTET, P., VERRECCHIA, K.E. & DUMONT, J.L. 1995. Spherulites in calcrete laminar  
789 crusts: biogenic CaCO<sub>3</sub> precipitation as a major contributor to crust formation. *Journal of Sedimentary*  
790 *Research*, **65**, 690-700.

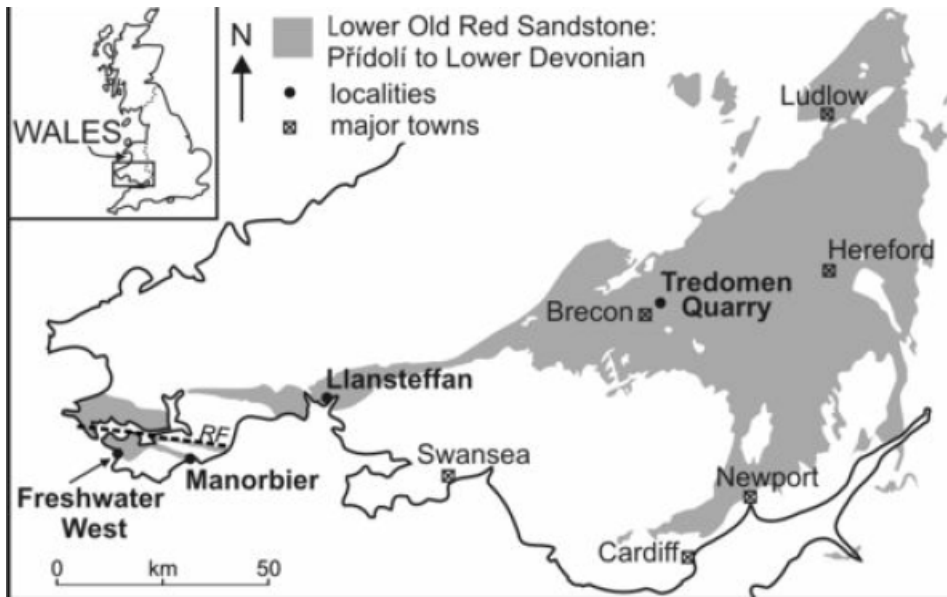
791 WHITICAR, M.J. 1999. Carbon and hydrogen isotope systematics of bacterial formation and oxidation of  
792 methane. *Chemical Geology*, **161**, 291-314.

- 793 WILDING, L., & TESSIER, L. 1988. Genesis of Vertisols: shrink-swell phenomena. *In: WILDING, L. &*  
794 *PUENTES, R. (eds) Vertisols: their distribution, properties, classification, and management.* A&M  
795 University Printing Center, College Station, TX, 55-79.
- 796 WILLIAMS, B.P.J. & HILLIER, R.D. 2004. Variable alluvial sandstone architecture within the Lower Old Red  
797 Sandstone, Pembrokeshire, UK. *Geological Journal*, **39**, 257-276.
- 798 WILLIAMS, B.P.J., ALLEN, J.R.L. & MARSHALL, J. D. 1982. Old Red Sandstone facies of the Pembroke  
799 Peninsula, south of the Ritec Fault. *In: BASSETT, M.G. (ed) Geological excursions in Dyfed, south-*  
800 *west Wales.* National Museum of Wales. Cardiff, 151-174.
- 801 WRIGHT, V.P. & MARRIOTT, S.B. 1996. A quantitative approach to soil occurrence in alluvial deposits and its  
802 application to the Old Red Sandstone of Britain. *Journal of the Geological Society, London*, **153**, 907–  
803 913.
- 804 WRIGHT, V.P. & TUCKER, M.E. 1991. Calcretes: an Introduction. *In: WRIGHT, V.P. & TUCKER, M.E. (eds)*  
805 *Calcretes.* Oxford, UK, Blackwell Scientific Publications, 1-22.
- 806 WRIGHT, V.P., PLATT, N.H., MARRIOTT, S.B. & BECK, V.H. 1995. A classification of rhizogenic (root-formed)  
807 calcretes, with examples from the Upper Jurassic–Lower Cretaceous of Spain and Upper Cretaceous of  
808 southern France. *Sedimentary Geology*, **100**, 143-158.
- 809 YAPP, C.J. & POTHS, H. 1994. Productivity of pre-vascular continental biota inferred from natural geothite.  
810 *Nature*, **368**, 49-51.

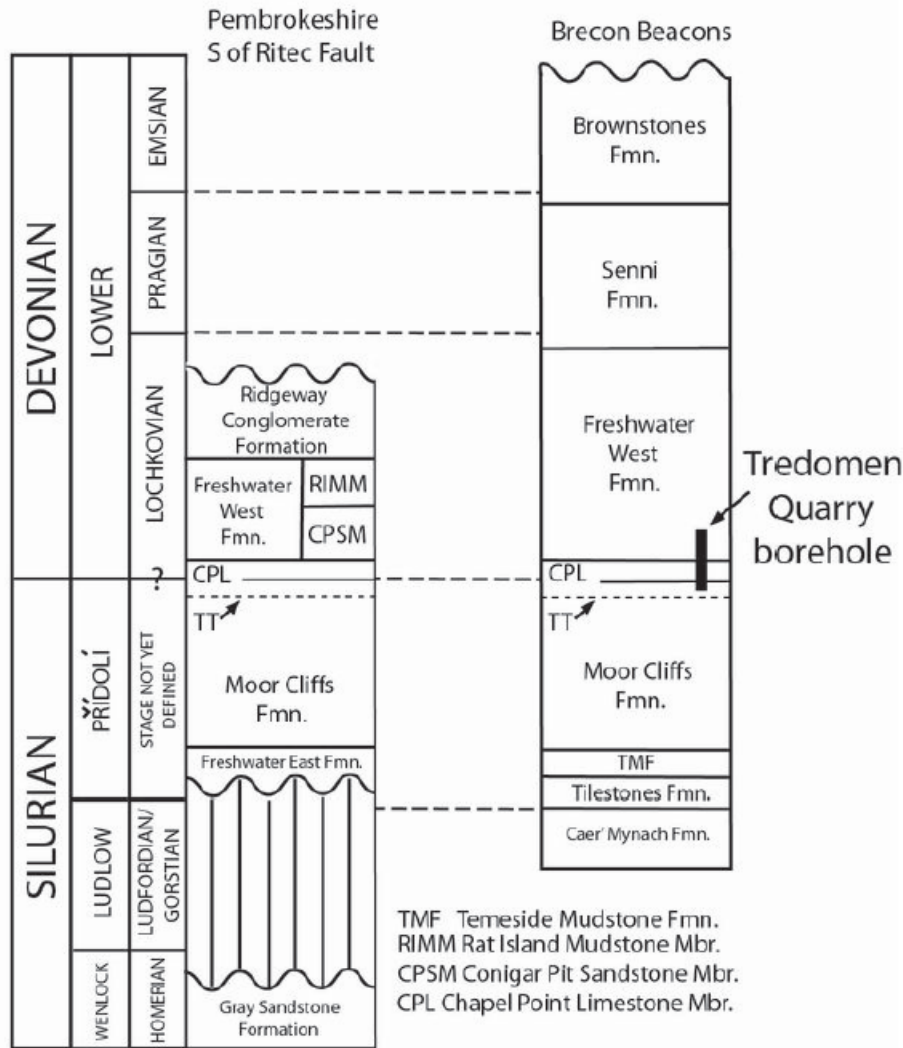
811

812 **Figure Captions**

813

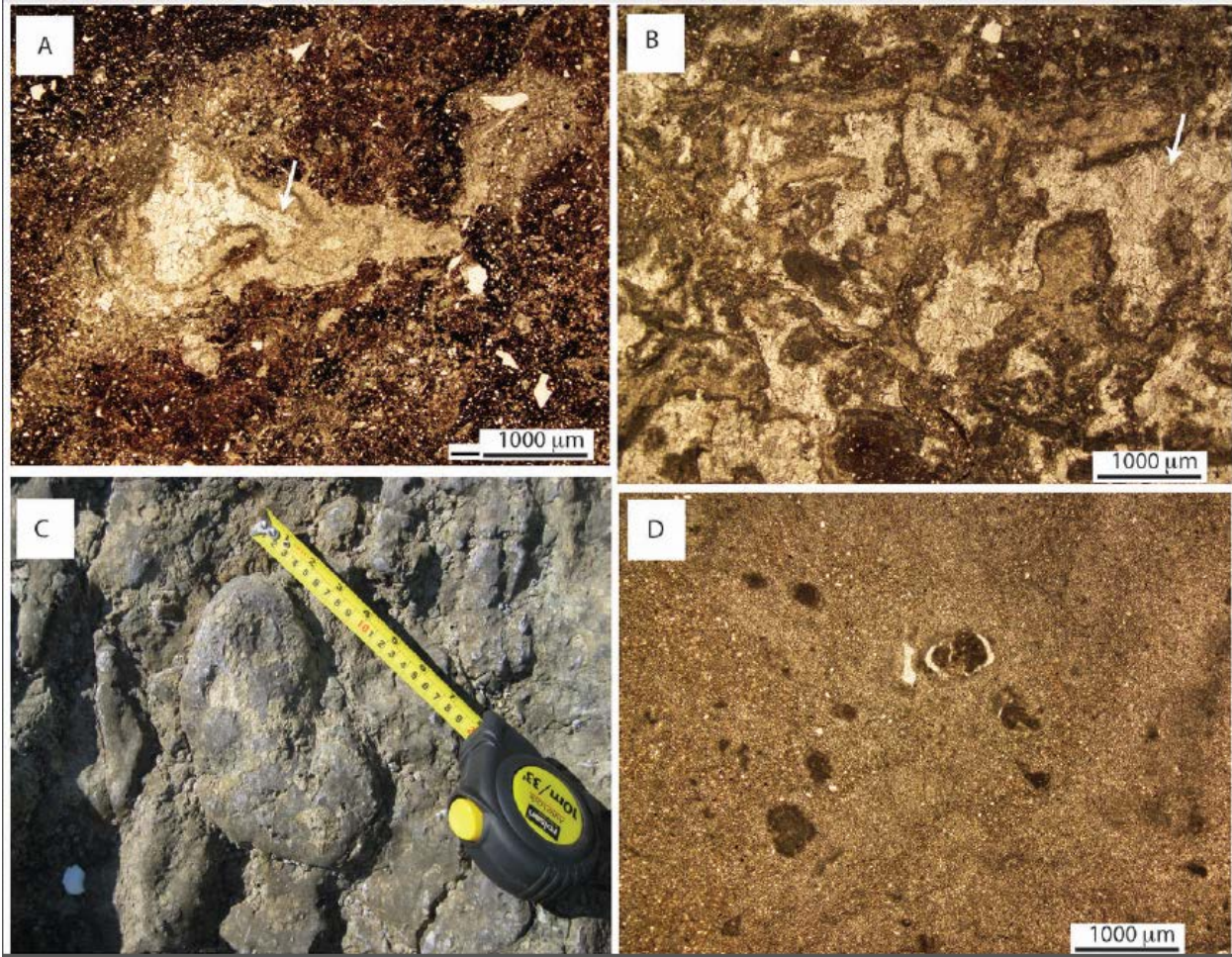


814  
 815 **Fig. 1.** Map showing the extent of the Lower Old Red Sandstone in South Wales and locations studied  
 816 (Freshwater West; Manorbier; Llansteffan; and Tredomen Quarry) RF = Ritec Fault. Inset map shows the  
 817 location of South Wales in the UK. Scale bar is 50 km.



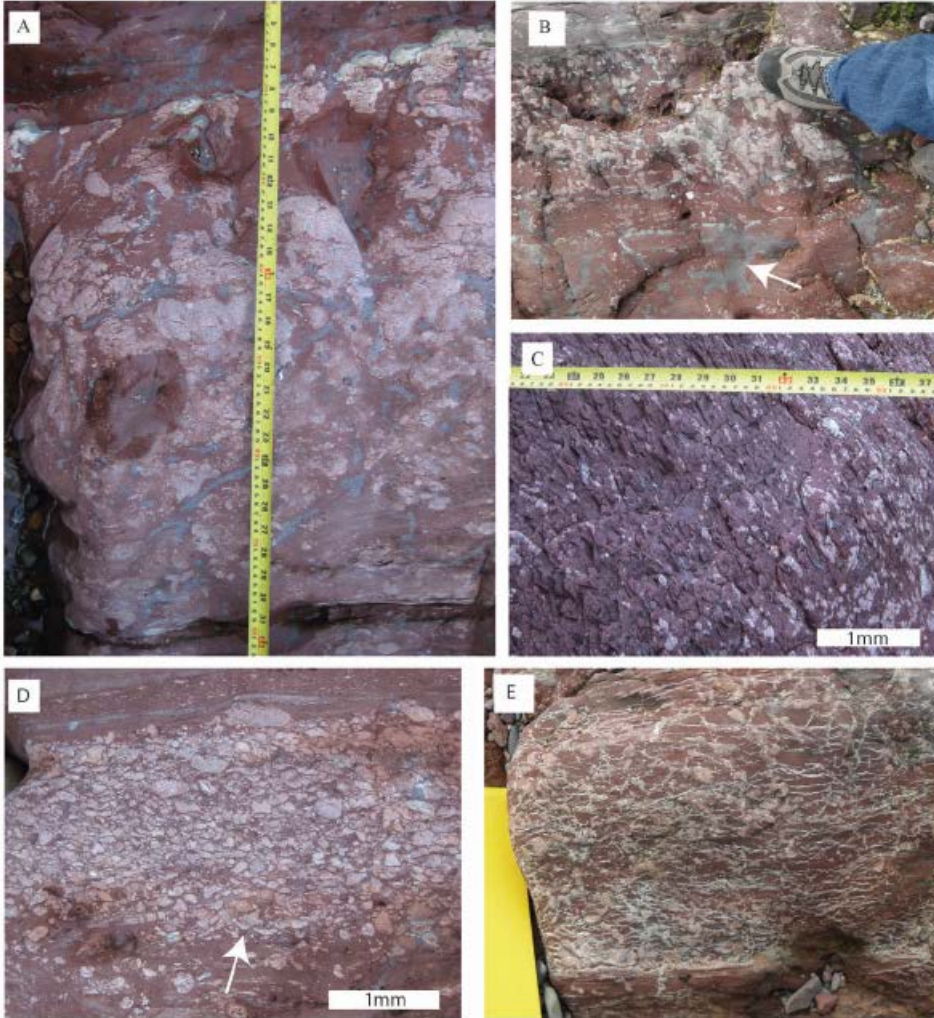
818

819 **Fig. 2.** Stratigraphic columns illustrating the studied formations of Lower Old Red Sandstone in  
 820 Pembrokeshire and Brecon Beacons; the Moor Cliffs Formation including the Chapel Point Limestone  
 821 Member (CPL) that outcrops above the Townsend Tuff (TT); the Conigar Pit Sandstone (CPSM) and Rat  
 822 Island Mudstone (RIMM) Members of the Freshwater West Formation; and the Ridgeway Conglomerate  
 823 Formation. The stratigraphic position of the core taken at Tredomen Quarry is also marked.



824

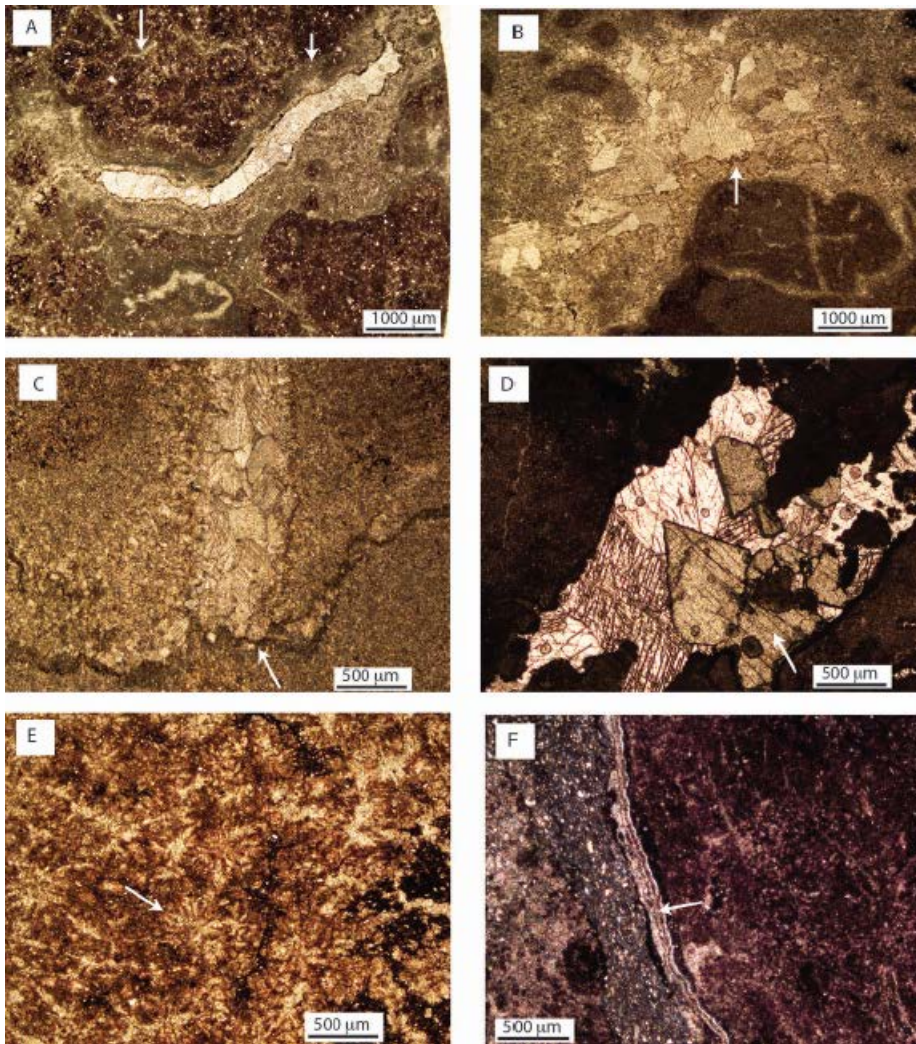
825 **Fig. 3.** Calcretes of the Moor Cliffs Formation. A) and B): Plane polarised light images of thin-section of  
 826 ATB MC 5 (an elongate, 15mm long and 3mm wide nodule from Manorbier), showing irregularly-shaped  
 827 patches of micrite that likely precipitated on an organic (perhaps plant root) substrate that was later (syn-  
 828 depositionally) oxidised, leaving a void that was infilled by clear calcite spar (arrowed). Note that the vertical  
 829 lines seen in the spar near the arrow are twin planes in the calcite spar, and not evaporite pseudomorphs. C): A  
 830 large, elongate (20 cm long, 10 cm wide), rounded nodule in the Chapel Point Limestone Member at  
 831 Llansteffan. D): A plane polarised light image of thin-section ATB 190810-01 (a 10 cm diameter nodule from  
 832 the Chapel Point Limestone Member at Llansteffan), showing the crystalline microspar mosaic and mm-sized  
 833 grains coated with clotted micritic fabrics. Scale bars in A, B and D are all 1000  $\mu\text{m}$ . Scale of the tape  
 834 measure in C is in cm (below) and inches (top).



835

836 **Fig. 4.** Outcrop images of the Freshwater West Formation. A) Large pedogenic nodules in a palaeo-Vertisol  
 837 of the Conigar Pit Sandstone Member at Manorbier (top of palaeosol is towards top of image). Scale on tape  
 838 measure is in inches (right side) and centimetres (left side). B) Palaeo-Vertisol with pedogenic calcrete  
 839 nodules and downward branching ‘drab haloes’ (arrowed) at Freshwater West. Note the palaeo-Vertisol has a  
 840 gradational base and truncated top. The boot is approximately 12 cm wide. C) Smaller nodules oriented  
 841 parallel to pedogenic slickensides in a Conigar Pit Sandstone Member palaeo-Vertisol at Manorbier (top of  
 842 palaeosol is to the right). D) Transported calcrete nodule clasts in a Conigar Pit Sandstone Member  
 843 conglomerate at Manorbier (arrow points to the base of the bed). E) Calcite-filled fractures interpreted as  
 844 pedogenic crystallaria in a palaeo-Vertisol at Freshwater West. The field of view is approximately 20cm from  
 845 top to bottom.

846

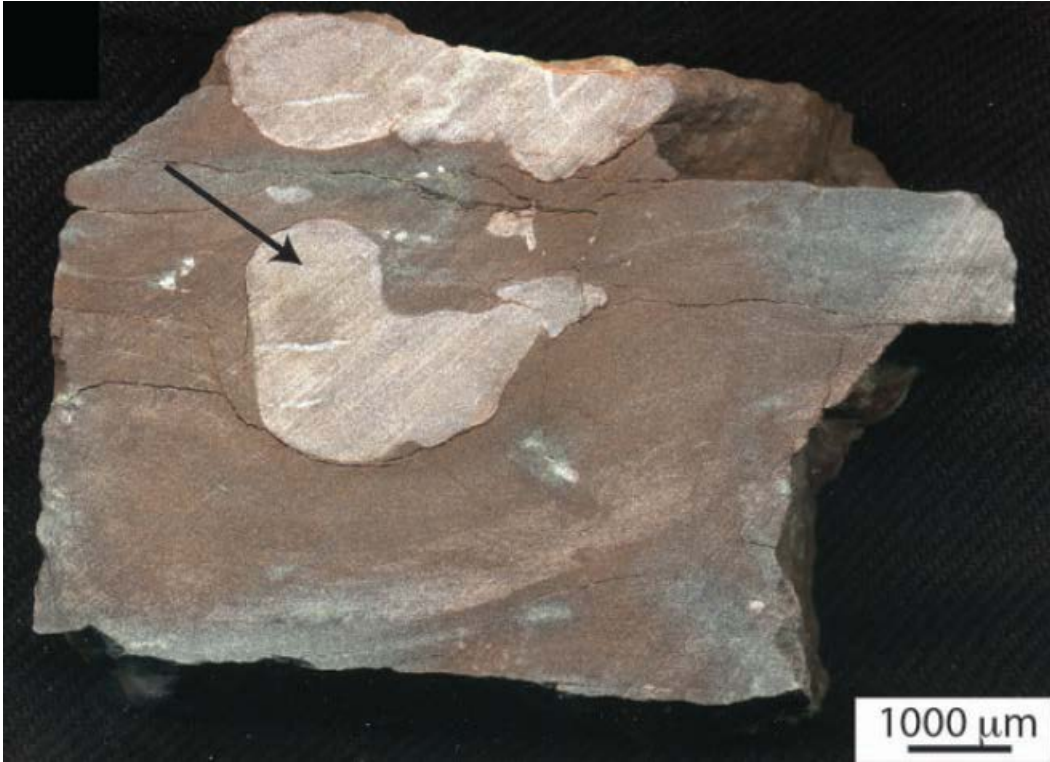


847

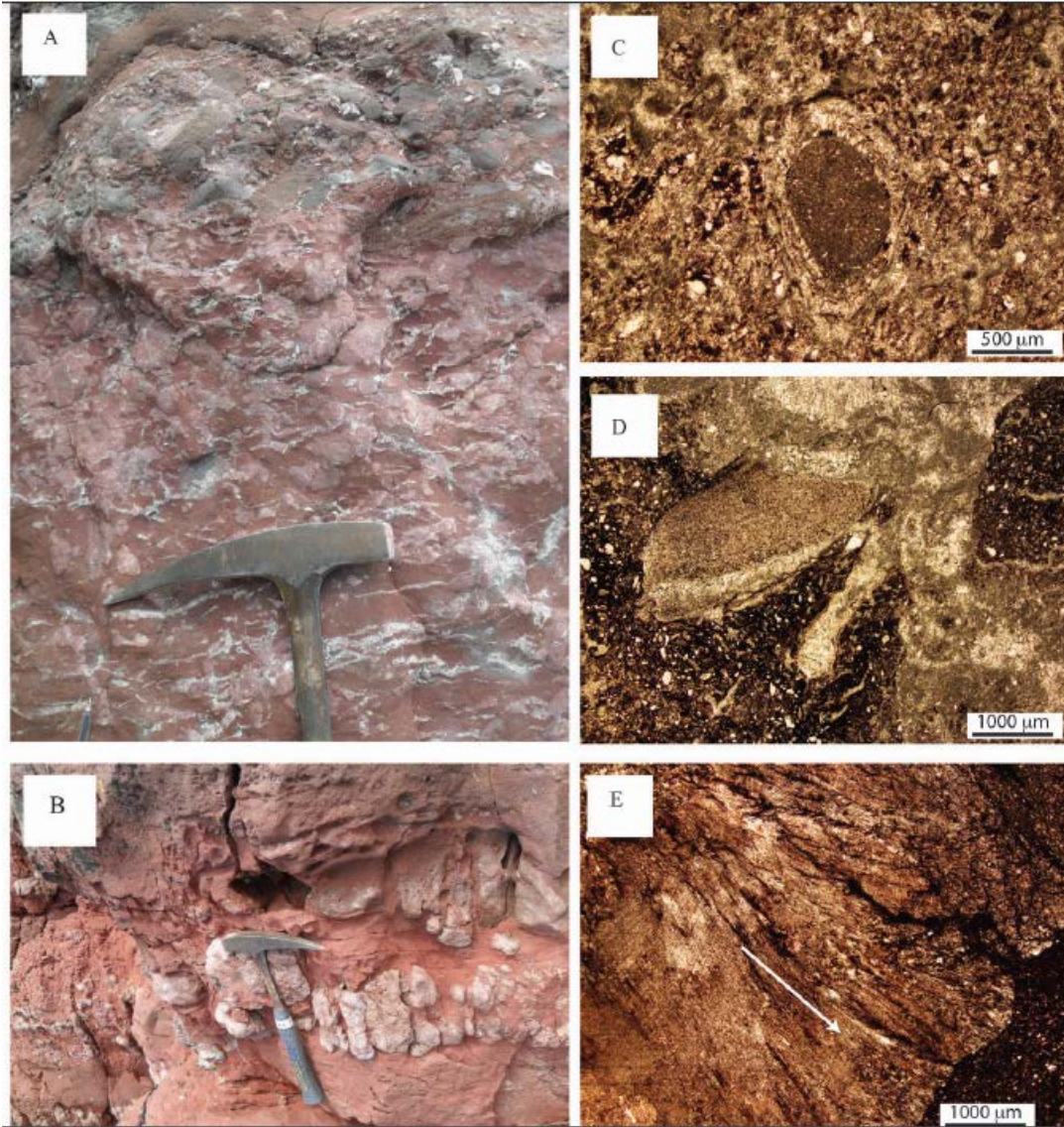
848 **Fig. 5.** Freshwater West Formation calcrites in thin-section. A) Thin-section of ATB 220810-05, a calcrite  
 849 nodule from the Conigar Pit Sandstone Member at Freshwater West. Clay-rich calcitic peloids amalgamated  
 850 into nodules, surrounded by central calcite spar-filled irregular and circumgranular cracks (left arrow), set in  
 851 matrices of haematitic clays and sub-angular quartz grains. The margins of the largest cracks are commonly  
 852 lined with a layer of dark micrite (right arrow). B) Thin-section of ATB 210810-11 (calcrite conglomerate  
 853 clast cut by crystallaria, from Conigar Pit Sandstone Member at Manorbier) showing stylolites (arrowed)  
 854 cutting across the circumgranular crack-filling spar. C) Thin-section of nodule ATB 220810-09 (Rat Island  
 855 Mudstone Member at Freshwater West) showing a uniform crystalline appearance. The matrix is cut by  
 856 stylolites (arrowed) and millimeter-scale ‘veinlets’ of sparry calcite. D) Thin-section of nodule ATB210810-7  
 857 showing dolomite or siderite rhombs (arrowed) in a fissure. E) Thin-section of nodule ATB 190810-7 from a  
 858 conglomerate in the Freshwater West Formation at Llansteffan, revealing spherulitic calcitic microspar. A  
 859 spherulite is arrowed. F) Laminar calcite crust of c. 100 microns thickness and c. 5mm length (arrowed)



860 around the outside of the spherulitic clast shown in D. Scale bars in A and B are 1000  $\mu\text{m}$ . Scale bars in C to F  
861 are 500  $\mu\text{m}$ .

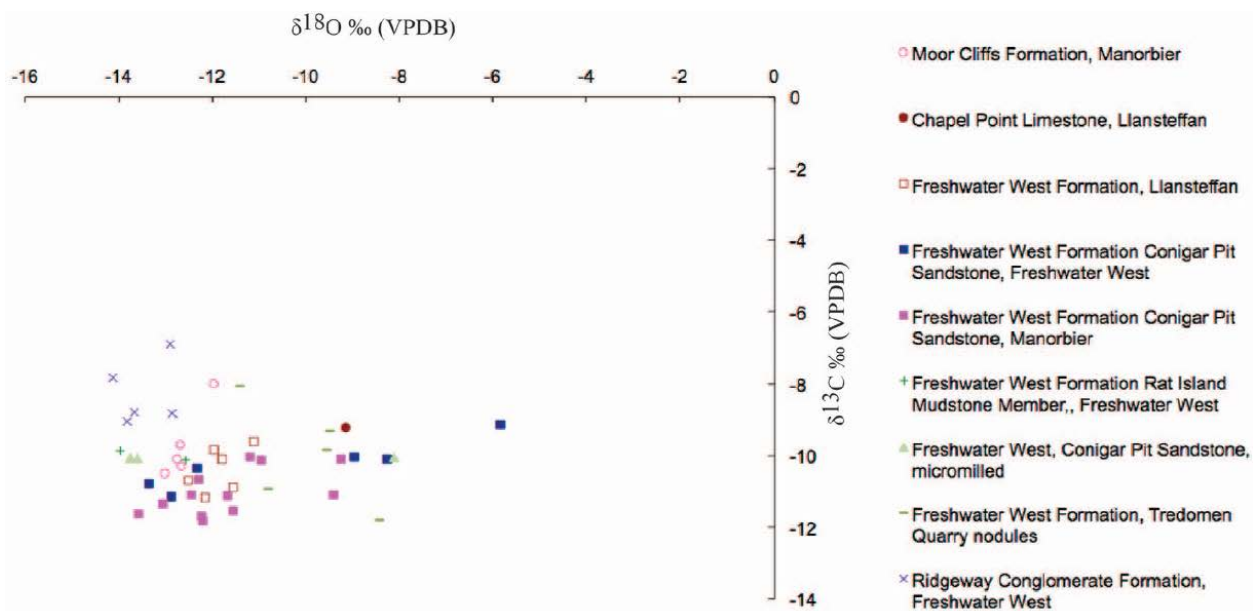


862  
863 **Fig. 6.** Calcrete nodule from Tredomen Quarry Core SO13SW/3 (BGS). A cut hand-specimen of nodule 1 is  
864 shown (arrowed; scale bar is 1000  $\mu\text{m}$ ).



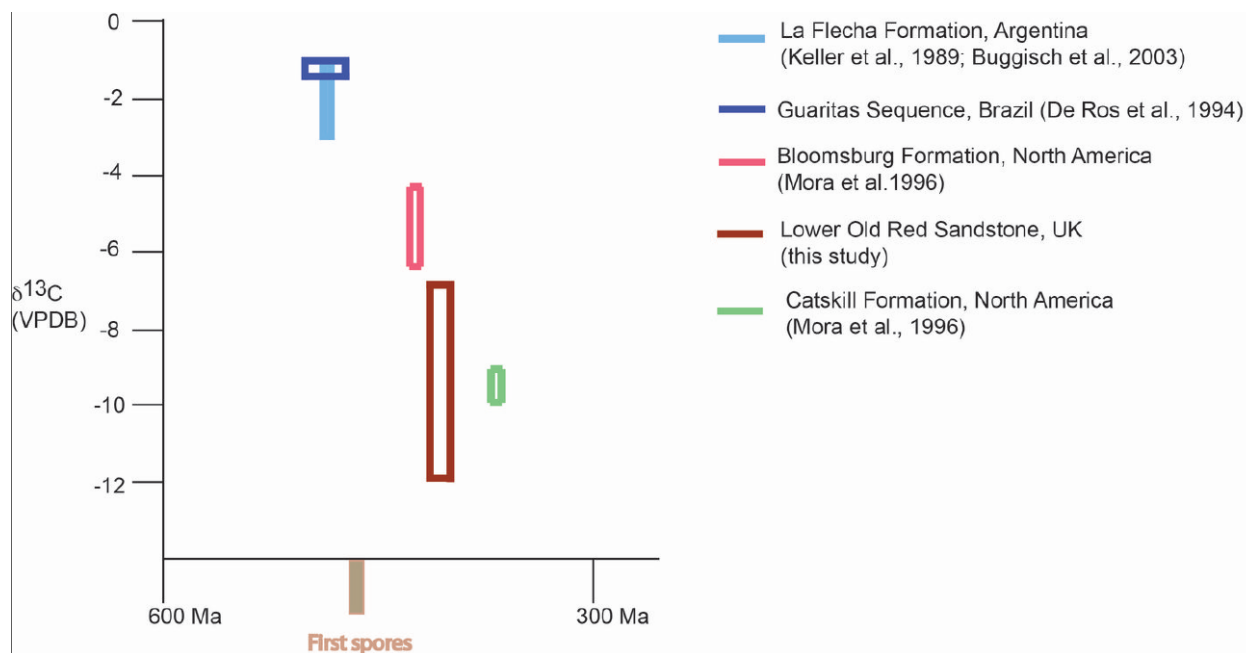
865

866 **Fig. 7.** Calcretes of the Ridgeway Conglomerate Formation at Freshwater West. A) Calcrete nodules and  
 867 crystallaria in a palaeo-Vertisol that is interbedded with alluvial fan conglomerates. B) Large, 10cm long and  
 868 layer-bound (groundwater calcrete?) nodules near the top of the Ridgeway Conglomerate Formation at  
 869 Freshwater West. C) A thin-section of nodule ATB 220810-11 revealing millimetre-sized dark micritic  
 870 peloids coated in c. 100 micron-thick layers of calcitic microspar. D) Patches of clear spar that infilled  
 871 millimeter-sized irregular cavities (burrows?) or cracks in thin-section ATB 220810-11. E) Image of thin-  
 872 section ATB 220810-13, from a very large c. 20 cm diameter nodule, part composed of curved columnar  
 873 calcite crystals These grew out from a reduction spot in the centre of the nodule (not visible in this image) into  
 874 the surrounding clay-rich matrix (arrow shows the direction of crystal growth). Hammer head for scale in A  
 875 and B is 17 cm wide; Scale bar in C is 500 µm, and 1000 µm in D and E.



876

877 **Fig. 8.** Cross-plot of carbon and oxygen isotopes for all calcrete samples measured. Overall calcrete  $\delta^{13}\text{C}$   
 878 values range from ca.  $-12\text{‰}$  to  $-6.9\text{‰}$ , and  $\delta^{18}\text{O}$  ranges from ca.  $-14\text{‰}$  to  $-5.8\text{‰}$ .



879

880 **Fig. 9.** Carbon isotopic compositions of selected Cambrian to Carboniferous calcretes. Very few data have  
 881 been published on late Cambrian to Silurian calcrete carbon isotopes (shown here). A representative selection  
 882 of data from Devonian and Carboniferous calcretes is given in this figure. This plot shows a transition from  
 883 calcretes with carbon isotopic compositions close to 0 per mil in the Late Cambrian, to calcretes with low  
 884  $\delta^{13}\text{C}$  (VPDB) compositions by the Late Silurian. This likely reflects different and evolving causes of

885 carbonate precipitation in terrestrial environments (e.g. 'common-ion effect' versus organic matter oxidation  
886 and CO<sub>2</sub> degassing).